energies

Article

Research on Optimal Operation of Power Generation and Consumption for Enterprises with Captive Power Plants Participating in Power Grid Supply–Demand Regulation

Hangming Liu [1], Huirong Zhao [1,*], Jincheng Yang [2] and Daogang Peng [1]

1 College of Automation Engineering, Shanghai University of Electric Power, Shanghai 200090, China; hangmingliu@outlook.com (H.L.); pengdaogang@shiep.edu.cn (D.P.)
2 Marketing Service Center, State Grid Xinjiang Electric Power Co., Ltd., Urumqi 830013, China; yang_jc1990@outlook.com
* Correspondence: hrzhao@shiep.edu.cn

Abstract: Wind and solar power curtailment and the difficulty of peak regulation are issues that urgently need to be addressed in the process of China's new electric power system. Enterprises with captive power plants (ECPPs) are large-capacity power consumers and producers, with significant optimization and adjustment potential on both the supply and demand sides. This paper aims to promote the active participation of ECPPs in grid supply–demand regulation and proposes an optimization model for the power generation and consumption of ECPPs based on a day-ahead, intra-day two-stage dispatching model. First, targeting demand response scenarios, mathematical models for analyzing the potential of ECPPs to participate in power grid supply–demand regulation are proposed. Then, an optimization model for ECPP generation and consumption with load regulation is established, and a two-stage dispatching model is proposed to fully mobilize the regulation flexibility of ECPPs. Finally, a robust dispatching model considering price uncertainty is established based on information gap decision theory. The case results show that ECPPs can reduce the curtailment rate in a region by approximately 9%, alleviate the peak pressure of the power grid, reduce carbon emissions by 1373.55 tons, and promote low-carbon development for themselves. Meanwhile, considering price uncertainty strengthens the risk resistance capability of ECPPs and provides a basis for their willingness to participate in supply–demand regulation.

Keywords: enterprises with captive power plants; supply–demand regulation; response demand; price uncertainty

check for updates

Citation: Liu, H.; Zhao, H.; Yang, J.; Peng, D. Research on Optimal Operation of Power Generation and Consumption for Enterprises with Captive Power Plants Participating in Power Grid Supply–Demand Regulation. *Energies* **2024**, *17*, 2106. https://doi.org/10.3390/en17092106

Academic Editor: Jay Zarnikau

Received: 1 April 2024
Revised: 22 April 2024
Accepted: 25 April 2024
Published: 28 April 2024

1. Introduction

With the high proportion of strongly fluctuating renewable energy in the power grid, traditional regulation resources have become insufficient to meet the demands of the safe and stable operation of the power system [1]. Therefore, developing and utilizing demand-side resources to participate in power grid supply–demand regulation has become an important task [2]. High-energy-consuming enterprises, which require a large amount of electricity during the production process, possess abundant adjustable resources and constitute an important part of demand-side resources [3,4]. These enterprises typically have captive power plants (CPPs) that generate electricity based on their load scale and production schedule [5,6]. In cases where self-generated electricity is insufficient, enterprises purchase electricity from the power grid [6,7]. These captive power plants have the advantages of small capacity, flexibility, and widespread distribution. By integrating the operation of high-energy-consuming enterprises and captive power plants with power grid supply–demand regulation, more efficient energy utilization and flexible power dispatch can be achieved [8,9].

Due to the high regulation flexibility of CPPs, there exists significant application potential in the fields of renewable energy accommodation and peak shaving auxiliary services [10,11]. Enterprises can actively participate in grid supply–demand regulation by flexibly adjusting the generation capacity and operating time of CPPs to meet the varying system power requirements in demand response scenarios [12]. Currently, the total installed capacity of CPPs nationwide has exceeded 156 million kilowatts. To alleviate the challenge of peak shaving and enhance renewable energy accommodation, it is necessary to fully explore the interactive potential of ECPPs in participating in power grid supply–demand regulation as well as electricity markets [13]. The interaction mode of ECPPs participating in the electricity market can refer to transactive energy systems (TESs) [14–16].

The operation mode and power supply characteristics of CPPs are not only related to the types and capacities of units but also to the industrial processes and electricity consumption characteristics of the enterprises [17,18]. The cooperative relationship between their production and operation should be taken into comprehensive consideration when tapping into the supply–demand regulation potential of ECPPs.

In current research on ECPPs dispatch optimization, Reference [19] considered a situation where the chemical industry has both cogeneration units and photovoltaic power generation, proposes a hybrid power resource optimization method, and determines the optimal operation mode. Reference [20] considered the probability of load loss and the stochastic characteristics of power generation and consumption to optimize the dispatching of maintenance plans for captive power plants. Reference [21] established a system dynamic simulation model to evaluate the impact of captive power generation on a cement plant's net emissions and expenditure through electricity use, under different scenarios for carbon-tax, grid emission factor, and electricity tariffs. Reference [22] proposed a leader-follower Stackelberg optimization model between leader and captive power plants, which aims to maximize the respective profits in the electricity market. Reference [23] utilized the method of system dynamics to optimize the cost of a textile industry with multiple fuel types of captive power plants, providing effective strategic decisions for enterprises. The above papers elaborate on the dispatching model of captive power plants but do not consider the impact of the internal source-load coupling of ECPPs.

As a special demand-side regulation resource, ECPPs can participate in the electricity market by selling their generation capacity. References [24,25] demonstrated the advantages of power generation rights trading between renewable energy units and captive power plants, enhancing the flexibility of the power system and improving the accommodation of renewable energy, which is beneficial for standardizing the operation of captive power plants. Reference [26] establishes a time-of-use pricing mechanism with a linkage between the supply side and the demand side to promote renewable energy accommodation, which is applied to the Western Inner Mongolia grid in China. Reference [27] proposes a mechanism for captive power plants to participate in the peak-shaving ancillary service market, which can effectively promote the consumption of renewable energy. The above references confirm the feasibility and economic benefits of CPPs participating in ancillary services in the electricity market. However, the existing dispatching models are unable to alleviate the imbalance between supply and demand caused by short-term forecasting errors within the day.

But for high-energy-consuming enterprises with captive power plants, existing research has not comprehensively considered the coupled relationship between the output of CPP units and the production load of the enterprises and has treated them as a unified entity; the optimization and regulation of specific demand response scenarios are not sufficiently clear. Meanwhile, the existing dispatching models do not adequately take into account intra-day optimization, thus limiting the full utilization of the regulatory potential of ECPPs. Furthermore, existing research has not considered the impact of price uncertainty on the cost and electricity consumption behavior of ECPPs, which leads to a risk of low or even zero willingness for ECPPs to participate in supply–demand regulation.

Information gap decision theory (IGDT) is a non-probabilistic and non-fuzzy approach that can quantify uncertainty in the absence of known information about uncertain variables. Reference [28] proposes a novel optimization framework based on IGDT for the strategic participation of multi-carrier systems in the electricity market under price uncertainty. Reference [29] presents a robust model for minimizing the cost of executing tasks by considering the uncertainty of the price of SVMs based on the IGDT; Reference [30] presents an energy management method for the interconnected operation of power, heat, and combined heat and power units to settle the day-ahead market in the presence of a demand response program. In summary, IGDT is an effective method for dealing with price uncertainty issues and can also be applied to ECPPs' participation in power grid supply–demand regulation.

Therefore, based on existing research, this paper proposes an optimization model of the power generation and consumption of ECPPs based on a day-ahead and intra-day two-stage dispatching model. First, potential mathematical models and regulation mechanisms are established based on source-load coupling constraints for different demand response scenarios. Subsequently, an analysis of the load regulation mechanism and its associated costs was conducted. With the objective of achieving optimal economic benefit, a bilateral collaborative optimization model for the power generation and consumption of ECPPs was constructed, accompanied by an improved dispatching mode. Finally, a robust scheduling model considering price uncertainty was developed based on IGDT. Through scenario comparisons, it was validated that the proposed optimization model based on the two-stage dispatching model can better alleviate the contradiction between supply and demand in the system, assisting enterprises in reducing costs and promoting low-carbon development. Simultaneously, by considering price uncertainty, the risk tolerance of ECPPs is enhanced to ensure its active participation in grid interactions, and it helps the grid system become aware of the changes in an ECPP's willingness to participate in supply–demand regulation during price fluctuations.

The main contributions of this paper are as follows:

(1) Based on different demand response scenarios, the analysis of ECPPs' regulatory strategies and the establishment of a mathematical model for their adjustment potential aids in evaluating and quantifying the demand response capabilities of ECPPs.
(2) An optimization model for power generation and consumption of ECPPs considering load regulation is established. This model can reduce the pressure on system peak shaving and renewable energy integration while promoting the low-carbon development of ECPPs, all while ensuring their economic benefits.
(3) The day-ahead and intra-day two-stage dispatching model described in this paper can better alleviate the supply–demand imbalance within the system and fully utilize the regulatory flexibility of ECPPs, and a segmented/sequential feedback solution strategy for optimization is proposed.
(4) Considering price uncertainty strengthens the risk resistance capability of ECPPs and provides a basis for the grid system, which become aware of the changes in ECPP's willingness to participate in supply–demand regulation during price fluctuations.

The organizational structure of this paper is as follows: Section 2 introduces the mechanism analysis of ECPPs participating in supply–demand regulation; Section 3 introduces the power generation and consumption optimization model, two-stage dispatching model and IGDT robust dispatching model; Section 4 analyzes and discusses the calculation examples; Section 5 provides the conclusion. The overall framework of this paper is shown in Figure 1.

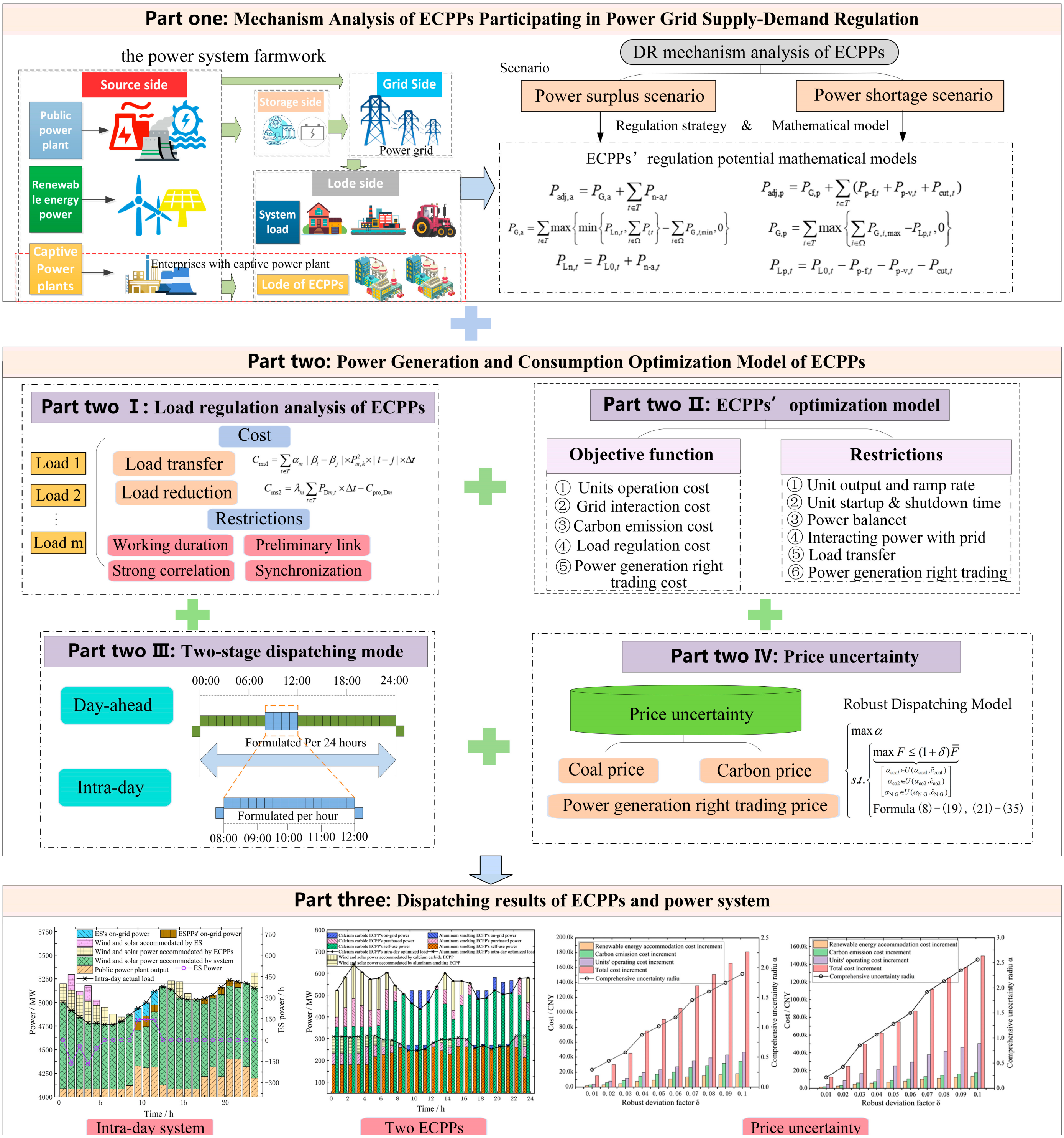

Figure 1. Overall framework diagram.

2. Mechanism Analysis of ECPPs Participating in Power Grid Supply–Demand Regulation

Based on the types of imbalances between power supply and demand in power grids, the scenarios where ECPPs participate in supply–demand regulation primarily include grid power surplus and grid power shortage. In both demand response scenarios, the regulatory potential of ECPPs is mainly influenced by their own adjustable capacity on both source-load dual-side, as well as the constraints of electricity coupling (the source side and load side mentioned in this paper refer to the CPPs and enterprise loads of the ECPPs, rather than the source side and load side of the power grid system).

2.1. Regulation Mechanism of ECPPs in the Power Surplus Scenario

A power surplus implies the existence of wind and solar power curtailment, which often occurs during the valley periods. To address the renewable energy curtailment issues, ECPPs participate in the supply–demand regulation of the power grid based on the regulation of source-load dual-side, utilizing demand response and power generation rights trading as their regulatory measures. The regulation mechanism is shown in Figure 2.

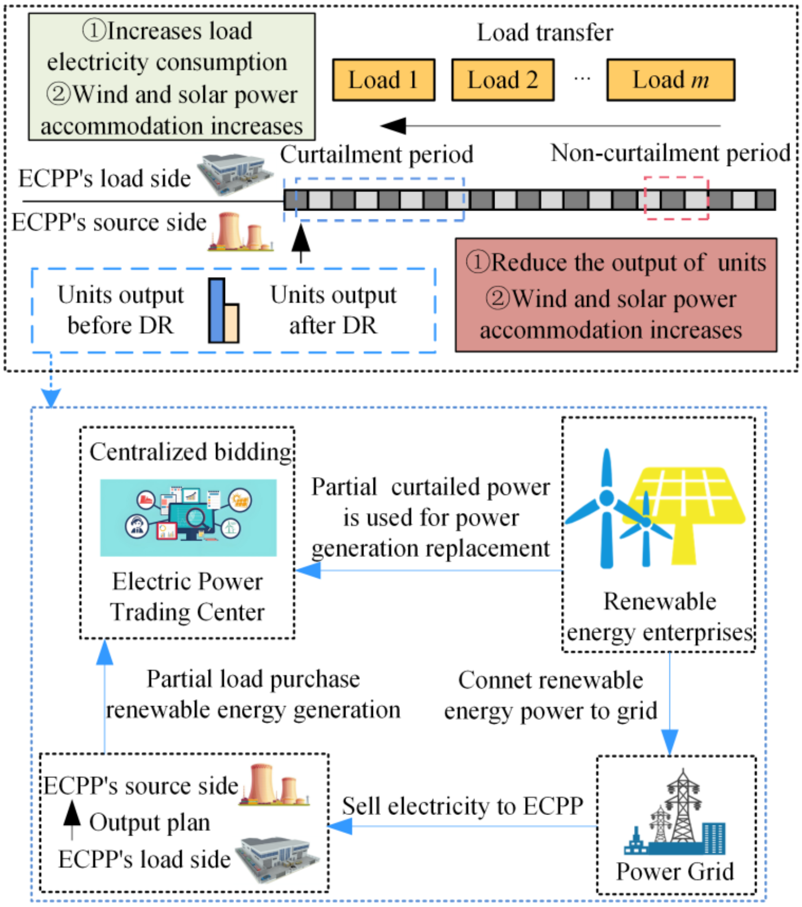

Figure 2. Regulation mechanism of ECPPs participating in the power surplus scenario.

On the demand side, high-energy-consuming enterprises regulate their operations through demand response, mainly in the form of load shifting. The adjusted load value after regulation is shown in Formula (1).

$$P_{\mathrm{Ln},t} = P_{\mathrm{L0},t} + P_{\mathrm{n-a},t} \quad (1)$$

where $P_{\mathrm{Ln},t}$ is the adjusted load value at time t during the power curtailment periods; $P_{\mathrm{L0},t}$ is the original load at time t; and $P_{\mathrm{n-a},t}$ is the load capacity shifted from non-curtailed power periods to curtailed power periods.

On the supply side, CPPs typically participate in the supply–demand regulation of power grid by power generation rights trading, which can effectively alleviate the system's peak-shaving pressure and enable the accommodation of curtailed electricity. Under this supply–demand regulation mode, CPPs reduce their output to create capacity for renewable energy accommodation, thus reducing energy consumption. Meanwhile, renewable energy enterprises increase their overall utilization hours of power generation, expanding the accommodation capacity for curtailed wind and solar power, and potentially receiving additional subsidies. Grid companies mitigate renewable energy curtailment issues and ensure the safe and stable operation of the power grid. The maximum adjustable power of the CPP is shown in Formula (2).

$$P_{\mathrm{G,a}} = \sum_{t \in T} \max\left\{ \min\left\{ P_{\mathrm{Ln},t}, \sum_{i \in \Omega} P_{i,t} \right\} - \sum_{i \in \Omega} P_{\mathrm{G},i,\min}, 0 \right\} \times \Delta t \tag{2}$$

where $P_{i,t}$ is the output of the i-th unit at time t; $P_{\mathrm{G},i,\min}$ is the minimum technical output of the i-th unit; Ω is the number of units; T is the total dispatching period, with a duration of 24 h; and Δt is the unit dispatching interval, with a duration of 1 h.

In conclusion, under the demand response scenario of a power surplus, the maximum adjustable power of ECPP is shown in Formula (3).

$$P_{\mathrm{adj,a}} = P_{\mathrm{G,a}} + \sum_{t \in T} P_{\mathrm{n-a},t} \times \Delta t \tag{3}$$

2.2. Regulation Mechanism of ECPPs in the Power Shortage Scenario

Power shortage often occurs during the peak periods. To alleviate the issue of peak shaving in the power system, ECPPs also participate in the supply–demand regulation of power grid based on the regulation of source-load dual-side, utilizing demand response and peak shaving by transmitting power to the grid as their regulatory measures. The regulation mechanism is shown in Figure 3.

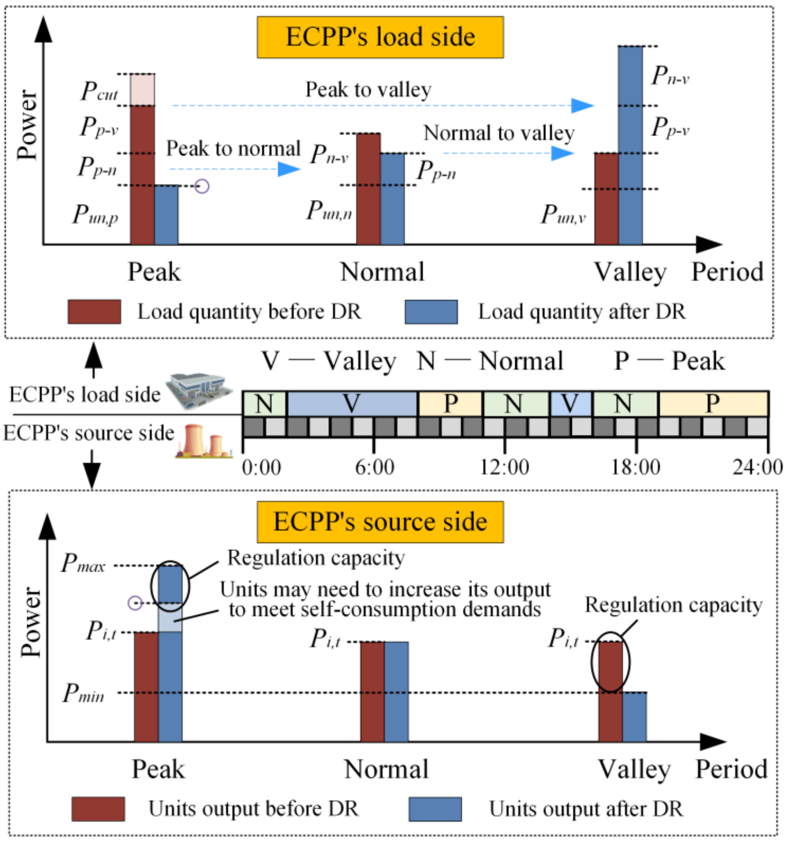

Figure 3. Regulation mechanism of ECPPs in the power shortage scenario.

On the demand side, high-energy-consuming enterprises regulate their operations through demand response, utilizing load shifting and load reduction to create additional capacity for peak shaving by CPPs. The adjusted load value after regulation is shown in Formula (4).

$$P_{\mathrm{Lp},t} = P_{\mathrm{L0},t} - P_{\mathrm{p-f},t} - P_{\mathrm{p-v},t} - P_{\mathrm{cut},t} \tag{4}$$

where $P_{\mathrm{Lp},t}$ is the adjusted load value at time t during the peak periods; $P_{\mathrm{p-f},t}$, $P_{\mathrm{p-v},t}$ are the peak-to-normal and peak-to-valley load shifting amount, respectively; and $P_{\mathrm{cut},t}$ is the load reduction amount at time t.

On the supply side, CPPs typically participate in the supply–demand regulation of power grid by power transmission for peak shaving. According to the "Guiding Opinions on Strengthening and Standardizing the Supervision and Management of Captive Coal-Fired Power Plants" issued by the National Development and Reform Commission and relevant regulations, gird-connected CPPs should comply with grid-dispatching management, provide peak shaving and other ancillary services to the power grid based on ECPPs' own load and unit characteristics, and systematically promote the participation of surplus capacity beyond self-consumption in the power market. The maximum adjustable power of the CPP is shown in Formula (5) as follows:

$$P_{\mathrm{G,p}} = \sum_{t \in T} \max\left\{ \sum_{i \in \Omega} P_{\mathrm{G},i,\max} - P_{\mathrm{Lp},t}, 0 \right\} \times \Delta t \tag{5}$$

where $P_{\mathrm{G},i,\max}$ is the maximum technical output of the i-th unit.

In conclusion, under the demand response scenario of power shortage, the maximum adjustable power of ECPP is shown in Formula (6).

$$P_{\mathrm{adj,p}} = P_{\mathrm{G,p}} + \sum_{t \in T} \left(P_{\mathrm{p-f},t} + P_{\mathrm{p-v},t} + P_{\mathrm{cut},t} \right) \times \Delta t \tag{6}$$

3. Power Generation and Consumption Optimization Model of ECPPs

3.1. Load Regulation Model and Cost Analysis of ECPPs

It is necessary to analyze the type of load composition in the period when load regulation of ECPPs is carried out during the dispatching period. In this paper, the load of each production link of ECPP is taken as the minimum unit. Let the set of production links of the ECPP be denoted as $S = \{S_1, S_2, \ldots, S_{\mathrm{M}}\}$, where M represents the total length of production links. The power flow relationship between the total power consumption $P_{\mathrm{L},k}$ and the load of production links of the ECPP is shown in Formula (7).

$$P_{\mathrm{L,k}} = P_{\mathrm{S1}} + P_{\mathrm{S2}} + \ldots + P_{\mathrm{SM}} \tag{7}$$

where P_{S1}~P_{SM} are the power consumption of each production link of the enterprise.

Production links can be divided into core production links and auxiliary production links; the core production links are crucial to an enterprise's production, such as the electrolysis process link in the aluminum-smelting industry, which is poorly regulable and can be used for a small amount of load reduction. Auxiliary production links are common in raw material processing links and finished product processing links, and they have higher rates of shiftability and reducibility.

3.1.1. Load Shifting Model of ECPPs

Load shifting is a regulation method based on price-driven demand response, essentially leveraging the time-of-use electricity price difference to reduce electricity costs.

The total load $P_{\mathrm{L},t}$ of the ECPP in the t-th operational assessment period is calculated as follows (the time period t in this paper refers to the period from time $t-1$ to time t):

$$P_{\mathrm{L},t} = P_{\mathrm{L0},t} + \sum_{i \in T} P_{\mathrm{L}(i,t)} - \sum_{j \in T} P_{\mathrm{L}(t,j)} \tag{8}$$

where $P_{\mathrm{L}(i,t)}$ is the load shifted from time period i to time period t; $P_{\mathrm{L}(t,j)}$ is the load shifted from time period t to time period j; and $P_{\mathrm{L0},t}$ is the original load in time period t.

$$P_{\mathrm{L0},t} = D_t + \sum_{m \in M} P_{m,t} \tag{9}$$

where D_t is the fixed load in regulation period t; $P_{m,t}$ is the m-th shiftable production link load in regulation period t.

In the actual production process, the shifting of production link loads is often constrained by temporal restrictions. Based on the sequentiality and process of the production links, the load shifting constraints are set as follows:

$$\sum_{t \in T} \theta_{m,t} = T_{m,z} \quad t \in [T_{m,\min}, T_{m,\max}] \tag{10}$$

where Formula (10) represents the working duration constraint of the production link load m; $T_{m,z}$ is the working duration of the production link load m; z is the entire time required to complete the production task; $T_{m,\min}$ and $T_{m,\max}$ are the upper and lower limits of the operating time of the production link load m; and $\theta_{m,t}$ is the coefficients of operating state, where 0 indicates interruption and 1 indicates operation.

$$\frac{1}{T_{m,z}} \sum_{t=1}^{t} \theta_{m,k} \geq \theta_{m,t} - \theta_{m,t+1} \quad \forall t \in T \tag{11}$$

$$\theta_{n,t} \leq \frac{1}{T_{m,z}} \sum_{t=1}^{t-1} \theta_{m,t} \quad \forall t \in T \tag{12}$$

$$\theta_{m,t} - \theta_{m,t+1} \leq \sum_{t=1}^{t-1} \theta_{n,t} \quad \forall t \in T \tag{13}$$

$$\theta_{n,t} = \theta_{m,t} \quad \forall t \in T \tag{14}$$

where Formula (11) represents the non-shiftable characteristic constraints of the production link load; Formula (12) represents the preliminary link constraint of the production link load, where the production link m can only start to work after the production link load n, which belongs to the same production process, has worked; Formula (13) represents the strong correlation constraint of the production link load, where the production link load m needs to start to work immediately after the production link load n has just completed the production task; and Formula (14) represents the synchronization constraint of the production link load, where the operating states of the production link loads n and m must remain the same.

The load shifting cost is typically related to the amount of shifted electricity and the duration of the shifting. Generally, as the load shifting takes longer, the cost of storing production materials and maintaining environmental conditions for ECPPs will be higher. Additionally, load regulation will lead to changes in power demand for enterprises. Since high-energy-consuming industries operate on a continuous shift basis, the additional labor costs caused by load shifting are negligible. The shifting cost of production link load m is as follows:

$$C_{\text{ms1}} = \sum_{t \in T} \alpha_m \left| \beta_i - \beta_j \right| \times P_{m,t}^2 \times \left| i - j \right| \times \Delta t \tag{15}$$

where α_m is the cost conversion coefficient of the production link load m; i and j represent the shifting of the production link load m between time i and time j; and β_i and β_j represent the proportion of electricity consumption of the production link load m within the total electricity consumption of the entire ECPP at time i and time j, respectively.

3.1.2. Load Reduction Model of ECPPs

ECPPs also have loads that can be reduced or even interrupted, and load reduction is regulated based on the incentive demand response.

The load reduction cost C_{ms2} of the production link load m is as follows:

$$C_{\text{ms2}} = \lambda_m \sum_{t \in T} P_{\text{D}m,t} \times \Delta t - C_{\text{pro,D}m} = (\lambda_m - \zeta_{\text{D}}) \sum_{t \in T} P_{\text{D}m,t} \times \Delta t \tag{16}$$

where $P_{\mathrm{D}m,t}$ is the load reduction of production link m; λ_m is the unit cost reduction coefficient of production link m; $C_{\mathrm{pro,D}m}$ is the reduction benefit of load reduction; and ζ_{D} is the unit compensation price. ECPPs are only willing to undertake load reduction when $\lambda_m - \zeta_{\mathrm{D}} < 0$, ζ_{D} varies depending on the urgency level of demand response.

$$P_{\mathrm{D}m,t} = \gamma_{\mathrm{D}m} P_{m,t} \mu_{m,t} \tag{17}$$

where $\gamma_{\mathrm{D}m}$ is the maximum allowable reduction rate of production link m, signifying load interruption when the value is 1; $\mu_{\mathrm{D}m}$ is the start–stop status coefficient for the load reduction demand response, where 1 indicates activation and 0 indicates no participation.

High-energy-consuming enterprises in different industries have different time limits for participating in load reduction; the relevant constraints on the reduction time are as follows:

$$\left(\mu_{\mathrm{D}m,t-1} - \mu_{\mathrm{D}m,t}\right)\left(T^{\mathrm{on}}_{\mathrm{D}m,t-1} - T^{\mathrm{on}}_{\mathrm{D}m,\min}\right) \geq 0 \tag{18}$$

$$\sum_{t \in T} \mu_{\mathrm{D}m,t} \leq \sum_{t \in T} T^{\mathrm{on}}_{\mathrm{D}m,\max} \tag{19}$$

where Formulas (18) and (19) represent the minimum and maximum time constraint for production link m to participate in load reduction, respectively; $T^{\mathrm{on}}_{\mathrm{D}m,t-1}$ is the load reduction duration of production link m up to time $t-1$; and $T^{\mathrm{on}}_{\mathrm{D}m,\min}$, $T^{\mathrm{on}}_{\mathrm{D}m,\max}$ are the minimum and maximum load reduction time for the production link m, respectively.

During load reduction, λ_m varies depending on the type of production process and the degree of reduction, which can be divided into three categories: (a) the continuous production of materials (reduction level 1); (b) maintenance of basic equipment operation with a cessation of material production (reduction level 2); and (c) shutdown of equipment (reduction level 3). In reduction level 1, material production is unaffected, resulting in a small reduction coefficient and making it the preferred option for load reduction. In level 2, further load reduction occurs with the cessation of material production while maintaining the minimum level of equipment operation. Consequently, an ECPP needs to bear additional costs for material loss. Compared to level 1, both λ_m and $\gamma_{\mathrm{D}m}$ increase. In level 3, the production process is completely shut down and interrupted, resulting in additional costs for equipment startup and shutdown damage, in addition to material loss costs. λ_m is the highest in this state while $\gamma_{\mathrm{D}m}$ is 1.

Due to the continuous production operations of high-energy-consuming enterprises, the equipment in their core production processes often operates with stable loads and cannot be interrupted. Interruptions can result in significant losses for the enterprise, including the risk of equipment scrapping. For example, in aluminum-smelting enterprises, the downtime of electrolytic cells in the electrolysis process generally cannot exceed 2 h, and the restart process requires the addition of fluxing agent cryolite and poses a high risk of scrapping, resulting in losses of up to 20 million CNY per hour for the enterprise. Therefore, reduction level 1 and 2 are usually considered. In the raw material processing and finished product manufacturing stages, the maximum reduction amount corresponds to the load power, and level 1, 2, and 3 can be taken into account.

3.2. Source-Load Power Generation and Consumption Optimization Model of ECPPs

3.2.1. Objective Function

Economic benefit is the primary factor that reflects the willingness of ECPPs to participate in demand response. Therefore, it is necessary to establish a model for the cost of power generation and consumption of ECPPs during the dispatch period, with the objective function being the minimization of the power generation and consumption costs of ECPPs.

$$\min C_{\mathrm{ECPP}} = C_{\mathrm{G}} + C_{\mathrm{B}} + C_{\mathrm{C}} + C_{\mathrm{S}} + C_{\mathrm{N}} \tag{20}$$

where C_{G} is the operating cost of the captive power plant; C_{B} is the interaction cost between ECPPs and the power grid; C_{C} is the cost of carbon emissions; C_{S} is the cost of load regulation; and C_{N} is the cost of the CPP participating in power generation rights trading. Among all the costs, C_{B}, C_{S} and C_{N} all belong to the costs involved in the interaction of power grid supply and demand.

(1) The operating cost C_{G} of the CPP

The operating cost C_{G} of the CPP units includes power generation cost C_{G1} and start-stop cost C_{G2}.

$$C_{\mathrm{G}} = C_{\mathrm{G1}} + C_{\mathrm{G2}} \tag{21}$$

$$C_{\mathrm{G1}} = \sum_{t\in T}\sum_{i\in\Omega}(a_i P_{i,t}^2 + b_i P_{i,t} + c_i) \times c_{\mathrm{coal}} \times \Delta t \tag{22}$$

$$C_{\mathrm{G2}} = \sum_{t\in T}\sum_{i\in\Omega}(1-\mu_{i,t})C_{si,t} \times \Delta t \tag{23}$$

where a_i, b_i, and c_i are the consumption constants of the i-th unit; c_{coal} is the real-time coal price; $\mu_{i,t}$ is the operating status coefficient of the i-th unit at time t, where 1 represents running and 0 represents shutdown; and $C_{si,t}$ is the boot cost of the i-th unit.

(2) The interaction cost C_{B} with the power grid

$$C_{\mathrm{B}} = \sum_{t\in T}(\mu_{1,t}P_{\mathrm{d},t} \times c_{\mathrm{d},t} - \mu_{2,t}P_{\mathrm{u},t} \times c_{\mathrm{u},t}) \times \Delta t \tag{24}$$

where $c_{\mathrm{d},t}$ is the off-grid price of ECPPs, which includes the system stand-by fee and government funds and surcharge of ECPPs; $P_{d,t}$ is the off-grid power of the ECPP; $c_{\mathrm{u},t}$ is the on-grid price of captive power plants; $P_{\mathrm{u},t}$ is the on-grid power of the captive power plant; and $\mu_{1,t}$ and $\mu_{2,t}$ are the interactive state coefficients of ECPPs.

(3) Carbon emission cost C_{C}

$$C_{\mathrm{C}} = \sum_{t\in T}[(k_{\mathrm{G},t}P_{i,t} + k_{\mathrm{d},t}P_{\mathrm{d},t}) \times \Delta t - M_{\mathrm{e}}] \times c_{\mathrm{co2}} \tag{25}$$

where c_{co2} is the trading price in the carbon emission market; M_{e} is the free emission quota of ECPPs; $k_{\mathrm{G},t}$ is the emission factor of the self-used electricity; and $k_{\mathrm{d},t}$ is the emission factor of the purchased electricity.

(4) Load regulation cost C_{S}

$$C_{\mathrm{S}} = C_{\mathrm{S1}} + C_{\mathrm{S2}} = \sum_{m\in M}(C_{m\mathrm{S1}} + C_{m\mathrm{S2}}) \tag{26}$$

where C_{S1} is the overall load shifting regulation cost of the ECPP; and C_{S2} is the overall load reduction cost of the ECPP.

(5) The cost C_{N} of the CPP participating in power generation rights trading

$$C_{\mathrm{N}} = \sum_{t\in T}(c_{\mathrm{N-G}} + c_{\mathrm{t,d}} + c_{\mathrm{gov}}) \times P_{\mathrm{N-G},t} \times \Delta t \tag{27}$$

where $c_{\mathrm{N-G}}$ is the power generation rights trading price, $c_{\mathrm{t,d}}$ is transmission and distribution tariff of the power grid, c_{gov} are the government funds and surcharges, and $P_{\mathrm{N-G},\,t}$ is the trading power, which is guaranteed acquisition. If the volume of curtailed electricity is inadequate or the actual power generated is less than $P_{\mathrm{N-G},\,t}$, the actual trading volume will decline accordingly.

3.2.2. Restrictions

(1) Unit output and ramp rate constraints

$$\mu_{i,t}P_{\mathrm{G},i,\min} \le P_{i,t} \le \mu_{i,t}P_{\mathrm{G},i,\max} \tag{28}$$

$$r_{i,\mathrm{d}} \le P_{i,\mathrm{t}} - P_{i,\mathrm{t}-1} \le r_{i,\mathrm{u}} \tag{29}$$

where $r_{i,\mathrm{d}}$, $r_{i,\mathrm{u}}$ are the ramp-down and ramp-up rates of the i-th unit, respectively.

(2) Unit startup and shutdown time constraints

$$t_{i,\text{on}}^{\min} \geq T_{i,\text{on}}^{\min} \quad t_{i,\text{off}}^{\min} \geq T_{i,\text{off}}^{\min} \tag{30}$$

where $t_{i,\text{on}}^{\min}$, $t_{i,\text{off}}^{\min}$ are the shortest startup and shutdown duration of the *i*-th unit during the dispatching period, respectively; $T_{i,\text{on}}^{\min}$, $T_{i,\text{off}}^{\min}$ are the shortest allowed start-up and shut-down time for the *i*-th unit, respectively.

(3) Power balance constraint of ECPPs

$$P_{\text{d},t} + P_{i,t} + P_{\text{N-G},t} = P_{\text{L1},t} \tag{31}$$

(4) Interacting power constraints with the power grid

$$\max\{P_{\text{d},t}, P_{\text{u},t}\} \leq P_{\text{c,max}} \tag{32}$$

$$\mu_{1,t} + \mu_{2,t} \leq 1 \tag{33}$$

where $P_{\text{c,max}}$ is the maximum interactive power between the ECPP and power grid. Formula (31) indicates that ECPPs cannot be on-grid and off-grid at the same time.

(5) Load shifting constraints

The load shifting constraints are shown in Formulas (8)–(19).

(6) The constraint of the CPP participating in power generation rights trading

$$P_{\text{N-G},t} \leq P_{\text{G,a},t} \tag{34}$$

where Formula (34) indicates the total trading capacity at time t cannot exceed the maximum regulated power of CPPs.

$$P_{\text{N-G},t} \leq \text{P}_{\text{W\&PV},t} + \text{P}_{\text{pub},t} - \text{P}_{\text{sys},t} \tag{35}$$

where $P_{\text{W\&PV},t}$ is the total output of renewable energy at time t, $P_{\text{pub},t}$ is the total output of public power plants at time t, and $P_{\text{Lsys},t}$ is the total system load at time t. Formula (35) indicates the total trading capacity at time t cannot exceed the maximum amount of renewable energy curtailment at that time.

3.2.3. Day-Ahead and Intra-Day Two-Stage Dispatching Model of ECPPs

Due to the high volatility of wind and solar power output, short-term fluctuations can severely impact the reliability of power supply or result in the waste of electric power resources. Therefore, this paper proposes a day-ahead and intra-day two-stage dispatching model for ECPPs, which contributes to the safe and stable operation of the power system, alleviates the imbalance between supply and demand caused by short-term forecasting errors of system sources and loads, and further stimulates the potential of ECPPs in supply–demand regulation. The two-stage demand response model of ECPPs mainly consists of day-ahead planning and intra-day execution, and the flowchart is shown in Figure 4.

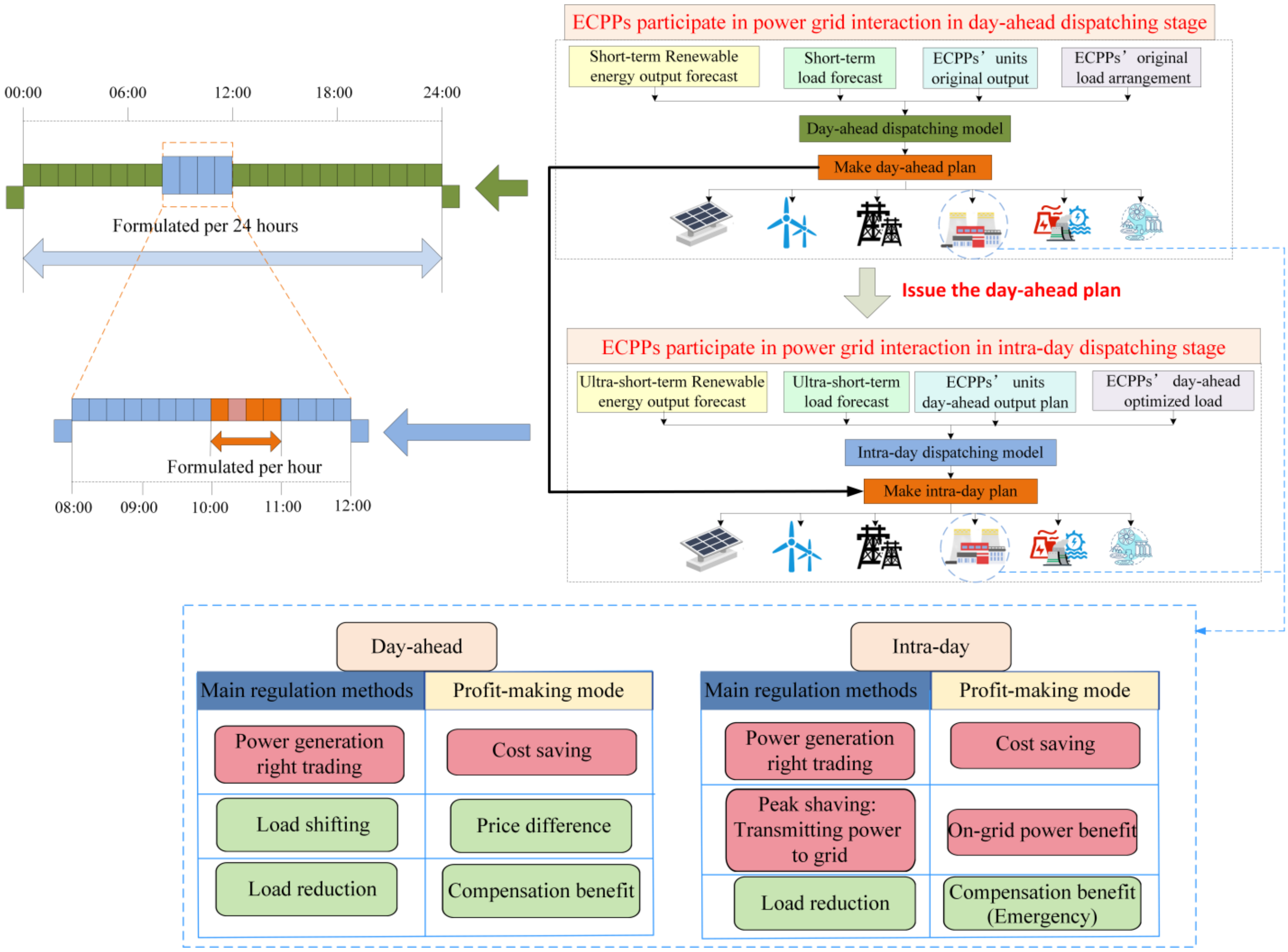

Figure 4. Two-stage dispatching flow chart of ECPPs.

In the day-ahead stage, a dispatching plan is formulated every 24 h. Each power entity of the power grid system reports data to the Electric Power Dispatching Center (EPDC); the EPDC acquires the predicted renewable energy output data, system load forecast data, as well as the planned output of ECPP units, load scheduling, and adjustable load conditions for the next day. The EPDC generates a dispatching plan that excludes the demand response of ECPPs and assesses whether the balance between supply and demand has been achieved.

(1) If the supply and demand of the power system have already reached a balance, there is no need to activate the demand response mechanism, and the aforementioned day-ahead plan will be issued as the official plan to each power entities.
(2) If there is a power shortage in the system after the output of the public power plant has been increased to its maximum capacity, the ECPPs will activate the demand response mechanism according to the regulation strategy outlined in Section 2.2 and based on power system requirements. The regulation methods include load shifting, load reduction, and peak shaving by transmitting power. The ECPP will carry out optimization dispatching of power generation and consumption and report the results to the EPDC. Subsequently, the EPDC will generate a day-ahead dispatching plan and issue the information to all power entities.
(3) If there is a power surplus in the system after the output of the public power plant has been reduced to its minimum, the ECPP will activate the demand response mechanism according to the regulation strategy outlined in Section 2.1 and based

on system requirements. The regulation methods will include load shifting and participating in power generation rights trading. Renewable energy enterprises first declare the trading information to the Electric Power Trading Center (EPTC), followed by ECPPs. After centralized bidding in the EPTC, the trading electricity quantity and price are determined, and the pre-clearing results are sent to the EPDC for power security verification. The specific trading process of the power generation right is shown in Appendix C. ECPPs perform internal optimal dispatching based on the system requirements and the regulation strategy in Section 2.1, report to the EPDC, and the EPDC generates and issues the day-ahead dispatching plan to complete the formal clearing of the power generation rights trading.

The corresponding electricity after the generation rights replacing needs to be purchased from the power grid, and the settlement is made either through a direct purchase agreement with renewable energy companies or according to the grid catalog tariff settlement; the settlement method of the region studied in the paper is the former.

During the intra-day actual operation, a dispatching plan is formulated every hour. Because of the short-time scale, only a small optimization is performed in the day-ahead dispatching plan. Due to the large scale, high flexibility, and cost-effectiveness of ECPPs in the studied region, as well as the need for ECPPs to undertake demand-oriented tasks such as balancing supply and demand, peak shaving, and renewable energy accommodation, ECPPs take priority in the optimized dispatching of various entities within the system through source-load regulation. When there are changes in the curtailed wind and solar power and the power shortage, the ECPPs needs to adjust their capacities of power generation rights trading and peak shaving by transmitting power based on their own actual conditions.

The superiority of the day-ahead and intra-day two-stage demand response dispatching model described in this paper for ECPPs and power grids lies in the following aspects:

(1) In the power shortages scenario, a huge power gap emerges due to the sudden decrease in wind and solar power output. Based on the new demand response model, ECPPs can perform emergency peak shaving according to their own source-load characteristics, thus reducing the peak shaving pressure on public power plants and avoiding power rationing or blackouts.
(2) In the power surplus scenario, the new demand response model enhances the matching degree of power generation rights trading capacity. The existing power generation rights trading is mostly monthly and annual based, which cannot solve the intra-day supply–demand imbalance contradiction caused by source-load forecast errors of the system. The power generation rights trading under the two-stage mechanism of ECPPs described in this paper belongs to a short-term trading mode, which can alleviate the contradiction between the medium and long-term trading mode and actual intra-day dispatching, as well as stimulate more of the supply–demand regulation flexibility of ECPPs.

The model and dispatch method proposed in this paper possess compatibility and reproducibility, which can be categorized into power entity expansion and power market similarity requirements as follows:

(1) In terms of ECPPs, the optimization model proposed in this paper has universal significance and can be applied to other industries as well as high-energy-consuming enterprises with other forms of self-supplied power.
(2) At the level of grid dispatch, Figure 4 can include more distributed energy resources (DERs), facilitating the expansion of the power system.
(3) In terms of the similarity of the electricity market, the application scenarios for the models and frameworks proposed in this article can be categorized under the concept of TESs. In TESs, prosumers can become sellers or buyers based on their own energy usage, representing a peer-to-peer (P2P) attribute of the electricity market. The models described in the article require a community-based P2P electricity market, where

participants cannot engage in direct transactions. Instead, a community manager serves as an intermediary, responsible for energy management and energy transactions. From the perspective of transaction models, this article involves both wholesale and bidding modes, which align with the transactional characteristics of TESs.

3.2.4. Solution Strategy and the Superiority

The solution method used in this paper is the Cplex solver based on the Matlab platform, which can handle the mixed-integer linear programming problems designed in this paper. There are two aspects of the dispatching issue: one is the internal generation and consumption optimization of ECPPs, and the other is the external optimization of ECPPs. During the optimization process, there is a problem of the "curse of dimensionality". Therefore, a directional optimization strategy is adopted in the internal generation problem of ECPPs, and a segmented/sequential feedback solution strategy is adopted to address the external optimization problem of ECPPs. The superiority of the solution method lies in its ability to reduce the search space for algorithm optimization and improve solution efficiency.

(1) The optimization of internal generation and consumption of ECPPs

This paper analyzes the regulation strategy of ECPPs in detail in Section 2, defining the optimization direction of ECPPs for two demand response scenarios that involve the essential characteristics of supply–demand imbalances. This is because only in this optimization direction can the economy of ECPP be better and meet the optimization goals of the power grid. Therefore, the optimization of both source and load sides within ECPPs has a certain direction, which can reduce the solution space for variables and increase the solution speed.

(2) Optimization outside of ECPPs (Grid's perspective)

From the perspective of the power grid, the optimization objectives include the requirements for high-quality power supply security, maximizing the accommodation of renewable energy, economic efficiency, and so on. Different optimization objectives are complementary and mutually exclusive, and the space dimension of multi-variable coupling solutions is large. As the system continues to connect with other DER entities, the difficulty of solving will increase, leading to the "curse of dimensionality" problem. This paper proposes a solution strategy based on "segmentation/sequence feedback". Each stage only optimizes part of the power entities to ensure that such entities play a maximum role, thereby achieving overall economy and stability. The optimization of each segment is related to the remaining load and relevant coupling variables. The specific steps are as follows:

$$\max G_{\mathrm{W\&PV}} = \sum_{t\in T} P_{\mathrm{W\&PV},t} \times \Delta t \tag{36}$$

$$\max \sigma_{\mathrm{PSP}} = \sqrt{1/T\sum_{t\in T}\left(P_{\mathrm{LPSP},t} - 1/T\sum_{t\in T} P_{\mathrm{LPSP},t}\right)^2} \tag{37}$$

$$\max C_{\mathrm{G,\ min}} = \left(\sum_{t\in T}\sum_{e\in N_E} C_{\mathrm{ECPP,\ min}} + \sum_{t\in T}\sum_{r\in N_R} C_{\mathrm{W\&PV}}\right) \times \Delta t \tag{38}$$

$$\min \sigma_{\mathrm{G,\ pub}} = \sqrt{1/T \times \sum_{t\in T}\left(\sum_{i\in N_{\mathrm{p}}} P_{\mathrm{pub},\ i,t} - 1/T \times \sum_{t\in T}\sum_{i\in N_{\mathrm{p}}} P_{\mathrm{pub},i,t}\right)^2} \tag{39}$$

$$\min C_{\mathrm{G,pub}} = \sum_{t\in T}\sum_{i\in \mathrm{N_p}} \left(a_i P_{\mathrm{pub},t}^2 + b_i P_{\mathrm{pub,t}} + c_i\right) \times c_{\mathrm{coal}} \times \Delta t \tag{40}$$

where σ_{PSP} the standard deviation of the remaining load after energy storage is connected to the grid; $P_{\mathrm{LPSP},t}$ represents the remaining load value after energy storage is connected to the grid.

Stage I: Optimization: Renewable energy power is prioritized for full integration into the grid to achieve the accommodation of renewable energy and clean energy substitution, in alignment with the economic objectives of grid operation, as shown in Formula (36). The equivalent residual load for each time period is then determined.

Stage II: Full accommodation of renewable energy may lead to imbalances in power supply and demand. Energy storage (ES) possesses flexible adjustment capabilities, providing dual functions of peak shaving and valley filling, making it cleaner than ECPPs. The optimization objective is shown in Formula (37), which aims to minimize the standard deviation of the remaining load after ES integration into the grid. The optimization results will be passed on to Stage III optimization.

Stage III: ECPPs and renewable energy enterprises, while ensuring economic efficiency, are encouraged to engage in power generation rights trading to smooth out the load curve after renewable energy integration into the grid. Additionally, due to the flexible regulation capabilities of CPPs, they can adjust power output more quickly and have lower operating costs compared to public power plants. Therefore, during this stage, it is desirable for public thermal power units to operate smoothly within the dispatching period, avoiding frequent startups, shutdowns, and adjustments. The overall objective is as shown in Formulas (38) and (39), and the equivalent residual load in each time period is obtained.

Stage IV: After the optimization in stage III, the imbalance between supply and demand caused by renewable energy integration into the grid is partially mitigated through the optimization of power generation and consumption by ECPPs. Therefore, the remaining load is assumed to be borne by public thermal power plants, and the overall objective is as shown in Formula (40).

The above four stages of optimization are carried out in sequence, with each stage optimizing only the same type of variables. This approach reduces the search space for algorithm optimization and improves the efficiency of the solution. However, during each stage of optimization, there may be issues with the dispatching failure of power entities. For example, in Stage III optimization, if the economic benefit of an ECPP is negative, the ECPP will have no willingness to participate in supply–demand regulation, resulting in no solution for this stage. Or if the change in load exceeds the ramping capability of public thermal power units, timely feedback is required for the optimization of Stages I–III. If no extreme situations occur in any scheduling period, feedback is not necessary.

Since this paper mainly focuses on the internal power generation and consumption scheduling of ECPPs and its participation in grid supply–demand regulation, the constraint conditions of DERs and public power units outside of ECPPs will not be further elaborated in this paper.

3.3. IGDT Robust Dispatching Model Considering Price Uncertainty

The source-load outputs of ECPPs can usually be planned and arranged by themselves, but there are great uncertainties in real-time coal price, carbon price, and power generation rights trading price. Dynamic changes in price factors will directly lead to changes in ECPPs' electricity consumption behavior; therefore, the set uncertainties of price model is established as follows:

$$\begin{cases} U(\alpha_{\text{coal}}, \widetilde{c}_{\text{coal}}) = \{c_{\text{coal}} : |c_{\text{coal}} - \widetilde{c}_{\text{coal}}| \le \alpha_{\text{coal}}\widetilde{c}_{\text{coal}}\} \\ U(\alpha_{\text{co2}}, \widetilde{c}_{\text{co2}}) = \{c_{\text{co2}} : |c_{\text{co2}} - \widetilde{c}_{\text{co2}}| \le \alpha_{\text{co2}}\widetilde{c}_{\text{co2}}\} \\ U(\alpha_{\text{N-G}}, \widetilde{c}_{\text{N-G}}) = \{c_{\text{N-G}} : |c_{\text{N-G}} - \widetilde{c}_{\text{N-G}}| \le \alpha_{\text{N-G}}\widetilde{c}_{\text{N-G}}\} \\ \alpha_{\text{coal}} \ge 0,\ \alpha_{\text{co2}} \ge 0,\ \alpha_{\text{N-G}} \ge 0 \end{cases} \tag{41}$$

where α_{coal}, α_{co2}, $\alpha_{\text{N-G}}$ are the uncertainty radii of coal price, carbon price, and power generation rights trading price; $\widetilde{c}_{\text{coal}}$, $\widetilde{c}_{\text{co2}}$, $\widetilde{c}_{\text{N-G}}$ are the possible future forecasting values of coal price, carbon price, and power generation rights trading price.

The comprehensive uncertainty radius of the prices is

$$\alpha = \omega_{\text{coal}}\alpha_{\text{coal}} + \omega_{\text{co2}}\alpha_{\text{co2}} + \omega_{\text{N-G}}\alpha_{\text{N-G}} \tag{42}$$

where ω_{coal}, ω_{co2}, $\omega_{\mathrm{N-G}}$ are the weight coefficients of the uncertainty radii of coal price, carbon price, and power generation rights trading price.

IGDT addresses the adverse effects of uncertain factors by defining robust functions, namely a risk aversion strategy. By setting the maximum uncertainty radius, the optimization objectives of the model are ensured to be limited within the tolerable risk levels. As the uncertainty radius value increases, the decision-making plan will be less affected by the fluctuation of uncertainty until it reaches a critical value, thereby improving the stability and risk tolerance of the model.

$$\begin{cases} \max\alpha \\ s.t. \begin{cases} \underbrace{\max F \leq (1+\delta)\overline{F}} \\ \begin{bmatrix} \alpha_{coal} \in U(\alpha_{\mathrm{coal}}, \widetilde{c}_{\mathrm{coal}}) \\ \alpha_{\mathrm{co2}} \in U(\alpha_{\mathrm{co2}}, \widetilde{c}_{\mathrm{co2}}) \\ \alpha_{\mathrm{N-G}} \in U(\alpha_{\mathrm{N-G}}, \widetilde{c}_{\mathrm{N-G}}) \end{bmatrix} \\ \text{Formulas (8)–(19), (21)–(35)} \end{cases} \end{cases} \tag{43}$$

where $\overline{F}$ is the optimal value of the objective function under the price certainty model; δ is the robust deviation factor, which represents the tolerable degree of risk for the ECPPs. The larger its value, the stronger the robustness of the model, which indicates that ECPPs can meet their own economic efficiency while participating in the regulation of power grid supply and demand.

Through analyzing the deterministic optimization model established previously, it can be observed that as coal prices, carbon prices, and generation rights trading prices increase, the total cost of the ECPPs tends to rise. Therefore, the model in Formula (38) can be simplified as the following single-layer model.

$$\begin{cases} \max\alpha \\ s.t. \begin{cases} F \leq (1+\delta)\overline{F} \\ \text{Formulas (8)–(19), (21)–(37)} \\ c_{\mathrm{coal}} = (1+\alpha_{\mathrm{coal}})\widetilde{c}_{\mathrm{coal}} \\ c_{\mathrm{co2}} = (1+\alpha_{\mathrm{co2}})\widetilde{c}_{\mathrm{co2}} \\ c_{\mathrm{N-G}} = (1+\alpha_{\mathrm{N-G}})\widetilde{c}_{\mathrm{N-G}} \end{cases} \end{cases} \tag{44}$$

4. Results and Discussions

4.1. Basic Data

This paper uses the power data of the regional power grid system (city level) in a northwest region of China for case analysis. The area contains two high-energy-consuming enterprises (calcium carbide and aluminum-smelting industries), a wind power plant, a photovoltaic power station, public power plants, and electricity loads within the grid system. The installed capacity and parameters of captive power plants, wind power plants, and photovoltaic power plants are shown in Appendix A Tables A1 and A2. The real time-of-use electricity price in the region is shown in Appendix A Table A3, and other price-related parameters are shown in Appendix A Table A4. The robust deviation factor δ is 0.02, and the weight coefficients ω_{coal}, ω_{co2}, $\omega_{\mathrm{N-G}}$ are 10, 1, 10, respectively. Energy storage in the form of pumped storage is adopted in this paper. The installed capacity of pumped storage is 300 MW, and the parameters are shown in Appendix A Table A6; the relevant constraints are shown in Appendix D.

Since the region has adopted the new energy bundling policy, new energy enterprises have unified quotations when trading power generation rights. The day-ahead dispatching plan excluding ECPPs' demand response in this area is shown in Figure 5. The real original load and planned unit output of the two ECPPs are shown in the pre-optimization data in Figure 6a,b. The production process flow of calcium carbide and aluminum-smelting enterprises is shown in Appendix B Figures A1 and A2. The two ECPPs dispatch independently in the optimization process.

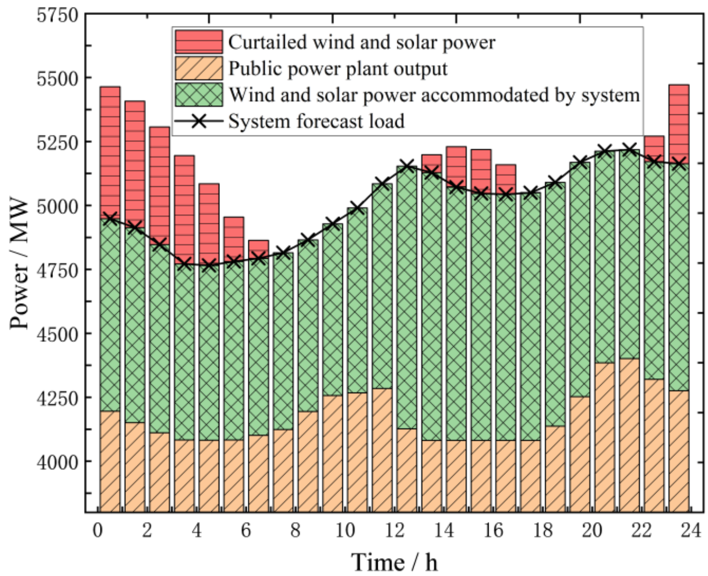

Figure 5. Original dispatching plan of the system.

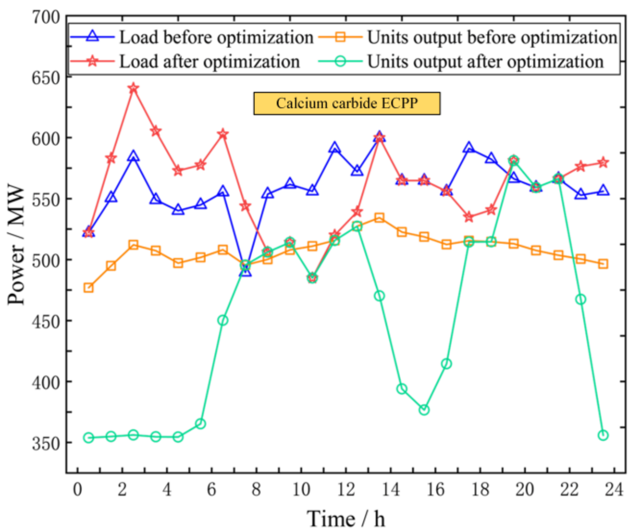

(**a**) Calcium carbide ECPP

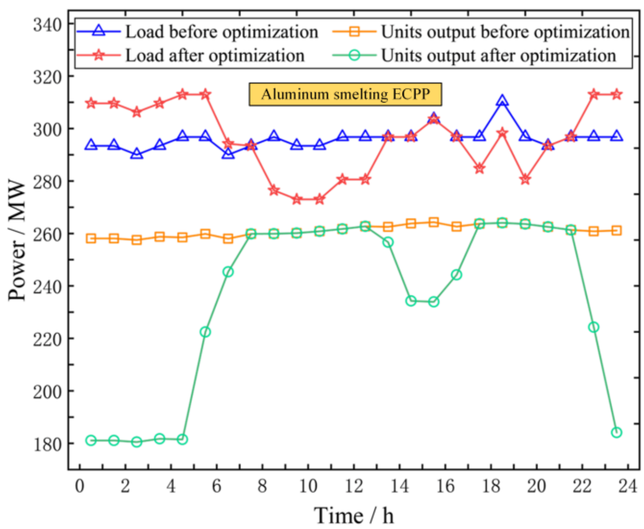

(**b**) Aluminum-smelting ECPP

Figure 6. Two ECPPs' data comparison.

In this paper, the following four scenarios are established. Through comparative analysis of the optimization results of each scenario, the superiority of the model described in this paper is verified.

Scenario 1: ECPPs do not participate in the supply–demand regulation of power grid and only optimize their own scheduling operations;

Scenario 2: ECPPs participate in the supply–demand regulation of power grid, adopting the traditional dispatching mode without considering intra-day generation and consumption optimization;

Scenario 3: ECPPs participate in the supply–demand regulation of power grid, adopting the day-ahead and intra-day two-stage dispatching model to optimize generation and consumption;

Scenario 4: The IGDT robust dispatching model considering price uncertainty is based on Scenario 3.

4.2. Deterministic Dispatching Results

Under the two-stage dispatching model described in this paper, the optimal dispatching of ECPPs and other power entities within the system is conducted, yielding the day-ahead and intra-day optimized dispatching results pertinent to Scenario 3.

4.2.1. Day-Ahead Optimization Dispatching Results

Based on the data presented in Figure 5 and Table A3, it is evident that power curtailment takes place between the hours of 22:00 and 7:00 the next day, which belongs to the power surplus scenario. Considering the control strategy discussed in Section 2.1, the primary focus of ECPP regulation involves load shifting and unit output.

The high-potential shifting load of aluminum-smelting enterprises mainly comes from alumina raw materials processing (Task 1) and aluminum profile processing (Task 2). Simultaneously, the shiftingable loads within carbide enterprises involve raw material processing (Task 3), carbide crushing and finished product processing (Task 4), and polyethylene polymerization (Task 5). Due to the fact that the aforementioned shiftingable loads pertain to raw material processing and the later-stage finished product processing, the tasks possess large shifting flexibility and are not bound by the limitations of T_{min} and T_{max}. Among the tasks, the storage of polyethylene in Task 5 demands stringent environmental conditions; therefore, it is not suitable for load shifting with a large time span. These tasks and related shifting parameters are shown in Table 1.

Table 1. Related parameters of load shifting.

Task Number	$P_{m,k}$/MW	$T_{m,t}$/h	α_m	Working Interval
1	4.17	10	100	6:00–20:00
2	12.2	14	10	0:00–24:00
3	14.8	9	10	6:00–20:00
4	32.7	11	5	0:00–24:00
5	23.6	10	10	0:00–24:00

Utilizing the day-ahead dispatching model alongside its constraints, load adjustments were conducted for tasks 1 through 5; the dispatching results of load shifting for the two ECPPs are graphically shown in Figure 7.

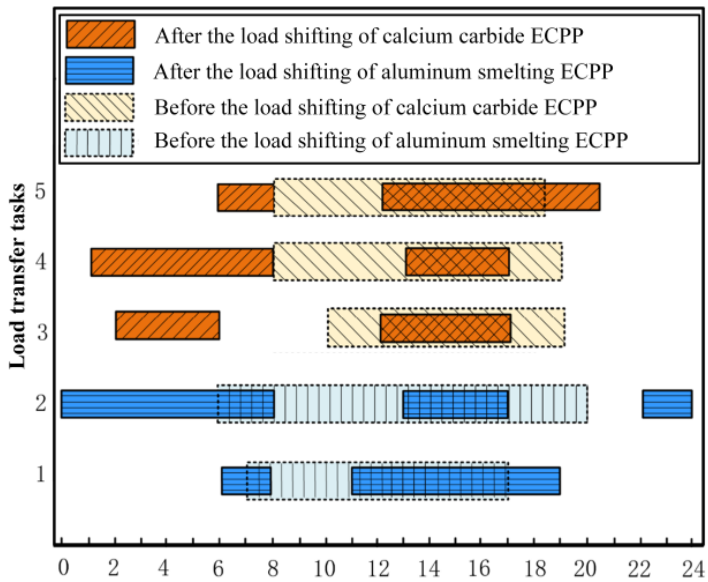

Figure 7. Load shifting situation of two ECPPs.

According to Figure 7, the shiftable loads of the two ECPPs mainly occur during 8:00–18:00. In calcium carbide ECPP, tasks 3–5 have time-sequential coupling constraints, and task 4 needs to be carried out first before task 5 can be carried out. Therefore, task 4 is concentrated in 1:00–8:00 in the dispatching results. The total shifting capacity of the aluminum-smelting ECPP and calcium carbide ECPP are 142.11 MW and 418.9 MW, respectively. The ECPPs' comparison data of load curves and unit output curves, before and after optimization of the day-ahead dispatching model, are shown in Figure 6a,b.

From Figure 6a,b, it can be observed that the loads of the two ECPPs during the period of 8:00–11:00 have been significantly reduced after optimization while the loads during the period of 22:00–7:00 have increased evidently, which achieves the function of peak shaving and valley filling and increase the accommodation of curtailed wind and solar power at the same time. The outputs of the ECPPs' units decrease to varying degrees in the 0:00–8:00 and 13:00–17:00 periods. The difference before and after optimization represents the accommodation capacity vacated by the captive power plants, which is the scope of power generation rights trading. The two ECPPs have cumulatively accommodated 2179.06 MW throughout the day, with the calcium carbide ECPP accommodating 1514.99 MW and the aluminum-smelting ECPP accommodating 664.08 MW.

Comparing the data from Figures 5 and 8, the overall system's power curtailment has decreased from 14.68% to 5.21% by ECPPs. In the day-ahead dispatching plan, the demand for system load has reached a supply–demand balance with public power plants and new energy plants during non-curtailed periods Therefore, the ECPPs' units adjust their output according to the load demand of ECPP as originally planned. Meanwhile the participation of PSP in optimized dispatch will further reduce the system's electricity curtailment rate. During the period from 23:00 to 5:00, the curtailed electricity will be nearly completely absorbed, while PSP replaces public fossil-fuel-fired power generation. The energy storage accumulates water for 7 h (1189.37 MW) to reach full generation capacity and generates electricity between 7:00–13:00 and 19:00–22:00.

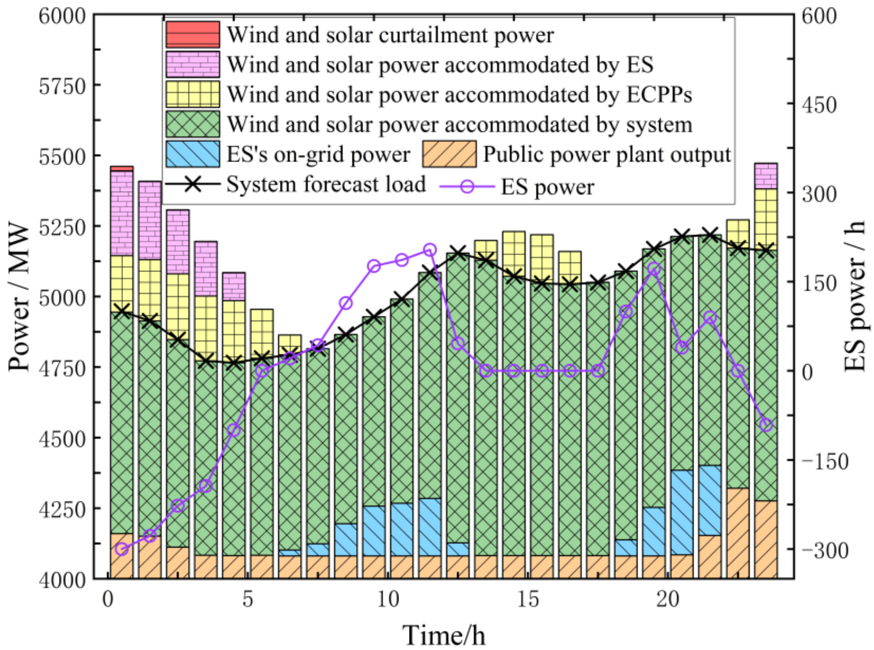

Figure 8. Day-ahead system optimization data.

4.2.2. Intra-Day Optimization Dispatching Results

During actual intra-day operation, the forecast errors of system load and renewable energy output can cause fluctuations in the supply–demand balance. Based on the dispatching model described in Section 3, the overall intra-day dispatching result is shown in Figure 9.

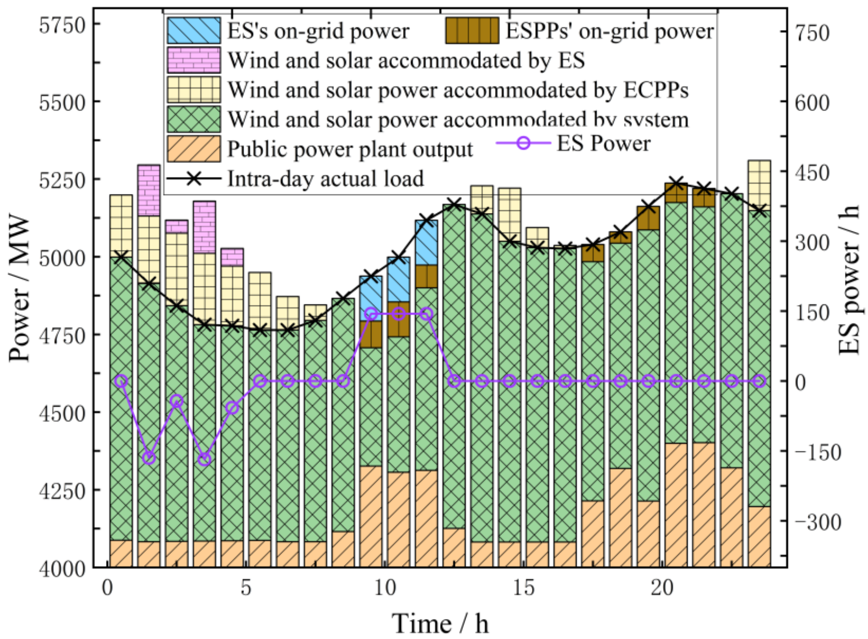

Figure 9. Intra-day system optimization data.

As can be seen from Figure 9, there is a certain deviation between the actual wind and solar power output and the predicted value during intra-day operation. If ECPPs do not participate in the power generation rights trading, the wind and solar power curtailment rate reaches 13.02%. According to the power generation rights trading results of day-before optimization, there has been a significant increase in the volume of wind and solar power curtailment. During the intra-day optimization, the trading volume of power generation rights between 15:00–17:00 and 22:00–0:00 decreased compared to the day-before level. This is because the reduced part can be accommodated by the system load, and the cumulative reduction is 371.65 MW.

During the period of 5:00–8:00 and 13:00–15:00, due to the available upward regulation capacity of the ECPPs' units, the cumulative increase in generation rights trading volume amounted to 82.14 MW. The overall trading volume showed a downward trend, which is attributed to the decline of the intra-day new energy output compared to the day-ahead forecast. In general, ECPPs can reduce the wind and solar power curtailment rate by 9.03% during the intra-day period.

During the period of 10:00–12:00 and 17:00–22:00, there is a power shortage in the system, and the ECPP performs flexibility peak shaving through demand response at this time. Since there is no volume for load shifting, the load needs to be reduced.

In the electrolytic process of aluminum-smelting ECPP, the electrolytic cell needs to maintain a high-temperature state and a certain thermal stability. In the practice of low-frequency load shedding for ECPP, 10% is the critical proportion of power reduction for continuous aluminum production and maintaining the heat preservation of the electrolytic cell. Similarly, this applies to the carbide furnace in calcium carbide ECPP. The unit cost reduction coefficients are set as 0.2; $T^{\mathrm{on}}_{\mathrm{D}m,\mathrm{min}}$ and $T^{\mathrm{on}}_{\mathrm{D}m,\mathrm{max}}$ are 0, 6. The remaining reduction parameters can be found in Appendix A Table A6.

During the periods of power shortage, the aluminum-smelting ECPP and calcium carbide ECPP can cumulatively reduce power consumption by 228.04 MW and 430.14 MW, respectively, freeing up a certain on-grid volume of ECPPs' units. Based on increasing their output to meet their own consumption needs, the two ECPPs can, respectively, deliver 119.39 MW and 445.38 MW of electric power to the power grid, which has alleviated the peak load regulation pressure on the power grid to a certain extent. The final optimized generation and consumption situation of the two ECPPs within the day is shown in Figure 10.

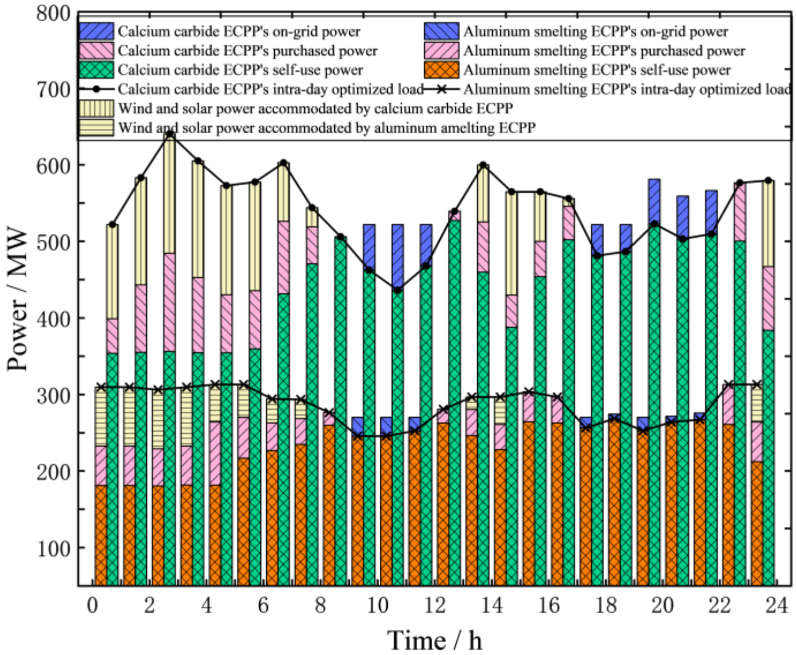

Figure 10. Actual intra-day power generation and consumption situation of ECPPs.

The curtailed electricity is fully absorbed by the further participation of the PSP, reducing the curtailment rate to 0%. PSP generates electricity between 8:00–13:00 and 17:00–23:00. This is because, compared to pumped storage, public fossil-fuel-fired power plants are more energy-consuming and costly power sources. With the participation of PSP, the generation of public fossil-fuel-fired power decreases. This is because energy storage represents a cleaner energy source, and it is therefore prioritized for grid connection in the EPDC, achieving 432.92 MW of generation.

Based on the data for that day, the integration of ES did not significantly impact the optimized electricity generation and consumption behavior of ECPPs. However, when the pumped water volume of the energy storage reaches a sufficient level, it may occupy the grid connection space of ECPPs, potentially reducing their revenue. Nevertheless, this satisfies the environmental protection requirements of the power system.

4.2.3. Comparative Analysis of Different Scenarios

According to the intra-day dispatching results, the contributions made by the two ECPPs to the regional power system and their own economic situations are shown in Tables 2 and 3, where Scenario 2 takes the average value based on medium and long-term trading data.

Table 2. Two ECPPs' contribution to the region in four scenarios.

Scenario Number	Industry Category	New Energy Accommodation/MW	On-Grid Power Supply/MW	Reduce Carbon Emission/t
1	Calcium carbide	-	-	-
	Aluminum smelting	-	-	-
2	Calcium carbide	1075.97	428.51	766.85
	Aluminum smelting	499.32	102.67	236.57
3	Calcium carbide	1354.94	445.38	766.85
	Aluminum smelting	577.36	119.39	606.7
4	Calcium carbide	1354.94	322.01	766.85
	Aluminum smelting	557.36	90.23	606.7

Table 3. Two ECPPs' cost composition in four scenarios.

Scenario Number	Industry Category	C_G/CNY	C_B/CNY	C_C/CNY	C_S/CNY	C_N/CNY	C_{sum}/CNY
1	Calcium carbide	1,588,083	635,494	185,988	-	-	2,409,565
	Aluminum smelting	1,179,440	408,958	97,823	-	-	1,686,211
2	Calcium carbide	1,446,162	359,501	172,326	68,354	135,516	2,181,859
	Aluminum smelting	1,039,266	337,847	95,673	35,802	60,572	1,569,160
3	Calcium carbide	1,404,830	260,901	161,444	41,703	151,594	2,020,472
	Aluminum smelting	1,008,738	229,182	87,190	20,694	72,456	1,418,260
4	Calcium carbide	1,413,805	279,072	170,669	41,736	155,323	2,060,605
	Aluminum smelting	1,021,936	243,245	84,740	20,648	75,354	1,445,923

As can be seen from Tables 2 and 3, comparing Scenario 1 with Scenario 2, the operating cost of Scenario 2 is significantly reduced. This is because the reduction in coal consumption after participating in power generation rights trading enables the ECPPs to operate in a low-energy consumption state, reduces carbon emissions, and lowers the overall cost of the ECPPs.

Comparing Scenario 2 with Scenario 3, the new energy accommodation of the two ECPPs has increased, respectively, but the accommodation cost has also risen accordingly. This is due to the increasing accommodation volume in Scenario 3. Based on the monthly actual trading volume, the trading volume of calcium carbide ECPP is 37.12 GW, with accommodation deviations of +3.89% and −17.5% under short-term trading mode and medium and long-term trading mode, respectively, and the trading volume of aluminum-smelting ECPP is 14.8 GW, with accommodation deviations of +2.09% and −17.7%, respectively. A comparison of the above data shows that the short-time scale generation rights trading mode can alleviate the contradiction between the medium and long-term trading mode and intra-day dispatching.

Comparing Scenario 3 with Scenario 4, the latter takes into account price uncertainty, and coal price, carbon price, and power generation trading price have increased, which has led to an increase in both its single and total cost. But the electricity consumption trend of ECPPs participating in the power generation rights trading has not changed, that is, it can still ensure cost reduction. However, due to the increase in coal prices and carbon prices, ECPPs' willingness of supplying power to grid has declined.

In summary, in cases where a power surplus exists, the units' output decreases, operating costs reduce, and carbon emission costs decrease after ECPPs participate in new energy accommodation; in cases where a power shortage exists, the unit operating cost increases, the grid interaction cost decreases, and the carbon emission cost increases after the ECPP participates in on-grid power supply. From the perspective of a single supply–demand regulation method, ECPPs are limited by the following factors when participating in power grid interaction.

(a) ECPPs will only have the willingness to participate in power generation rights trading when the sum of new energy accommodation cost, units operating cost, and carbon emission costs after participating in the power generation rights trading is less than the sum of units operating costs and carbon emission costs before the transaction. In this process, the power generation rights trading price and coal price are uncertain key influencing factors.

(b) ECPPs will only have the willingness to participate in on-grid power supply when the sum of unit operating cost, power grid interaction cost, and carbon emission costs after participating in on-grid power supply is less than the sum of the above costs before the participation. In this process, the coal price and carbon price are uncertain key influencing factors.

Therefore, it is necessary to conduct uncertainty analysis on these factors.

4.3. Influence of Price Uncertainty on Dispatching Results

In this paper, the robust deviation factor is taken to be 0.02, and the weight coefficients of uncertainty radii of coal price, carbon price, and power generation trading price are 10, 1, and 5. Using the risk aversion strategy to optimize the total cost of calcium carbide ECPP based on the IGDT robust model, the final total cost is F = 2,060,605 CNY, and the uncertainty radius of coal price, carbon price, and power generation rights trading price are 0.0063, 0.0571, and 0.0246. It shows that when the actual value of coal price fluctuates within 6.3%, the carbon price fluctuates within 5.71%, and the power generation rights trading price within 2.46%, the total dispatching cost of the system will not exceed 2,060,605. Similarly, for aluminum-smelting ECPP, F = 1,445,923 CNY, and the uncertainty radii are 0.013, 0.036, and 0.04.

4.3.1. The Effect of the Robust Deviation Factor on Dispatching Results of the IGDT Model

To delve deeper into the influence of price uncertainty on the cost and willingness of ECPPs to participate in supply–demand regulation, an analysis was conducted with varying parameter values for the robust deviation factor. The trends of uncertainty radius, units' operation cost, the carbon emission cost, new energy accommodation cost, and the ECPPs' total cost of the uncertainty model are shown in Figure 11 by setting the robust deviation factor to vary in 0–0.1.

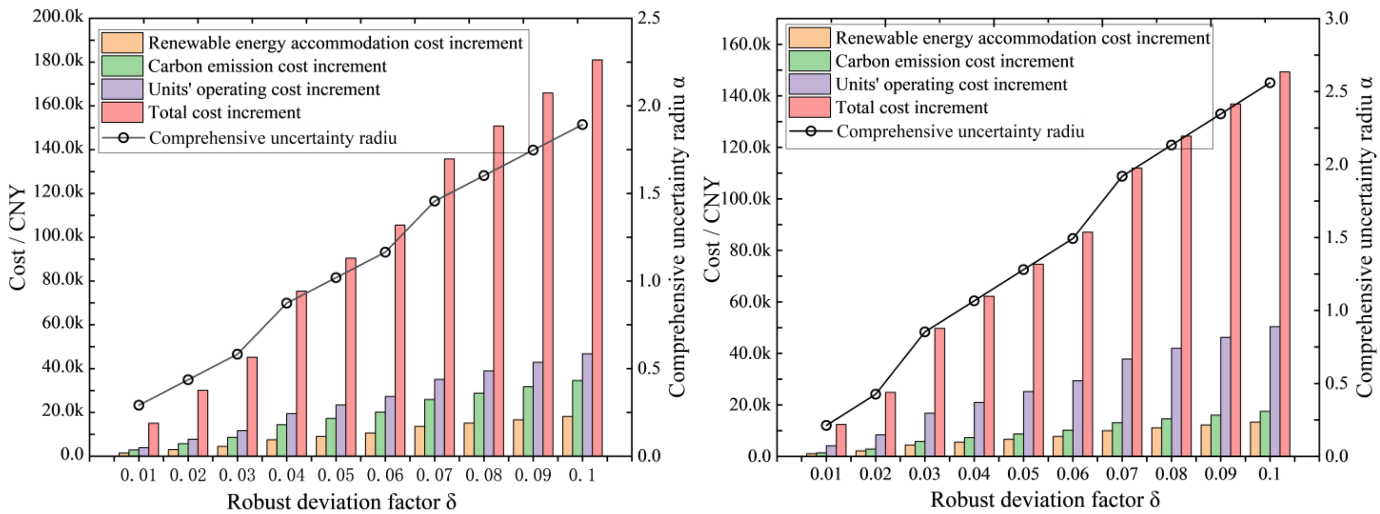

Figure 11. Trends of costs and uncertainty radius of ECPPs.

As shown in Figure 11a,b, as the robust deviation factor increases, the comprehensive uncertainty radius continues to grow. ECPPs' renewable energy accommodation cost, units operating cost, carbon emission cost, and total cost all increase. This is because the robust model under the risk aversion strategy makes it so that price uncertainty can push the target expectation of ECPPs in an unfavorable direction, leading to an increase in both single and total costs for ECPPs.

For ECPPs themselves, a larger uncertainty radius reduces the impact of price uncertainty on ECPPs' economic benefits, improving ECPPs' ability to withstand price uncertainty. This allows ECPPs to always optimize towards lower total costs. Therefore, an ECPP can select an appropriate deviation factor based on the costs it can afford.

But for the power grid system, price uncertainty will lead to changes in ECPPs' electricity consumption behavior. From the trend of ECPPs' power generation and consumption, it can be seen that as the robust deviation factor increases, ECPPs' on-grid power supply and on-grid revenue gradually decline. This is because the increase in coal price and carbon price leads to an increase in the cost of ECPPs' upward power generation, and with the fixed benchmark electricity price of thermal on-grid power, ECPPs' willingness to supply power to the grid gradually decreases; the economic efficiency trends of ECPPs supplying power to grid are shown in Figure 12a.

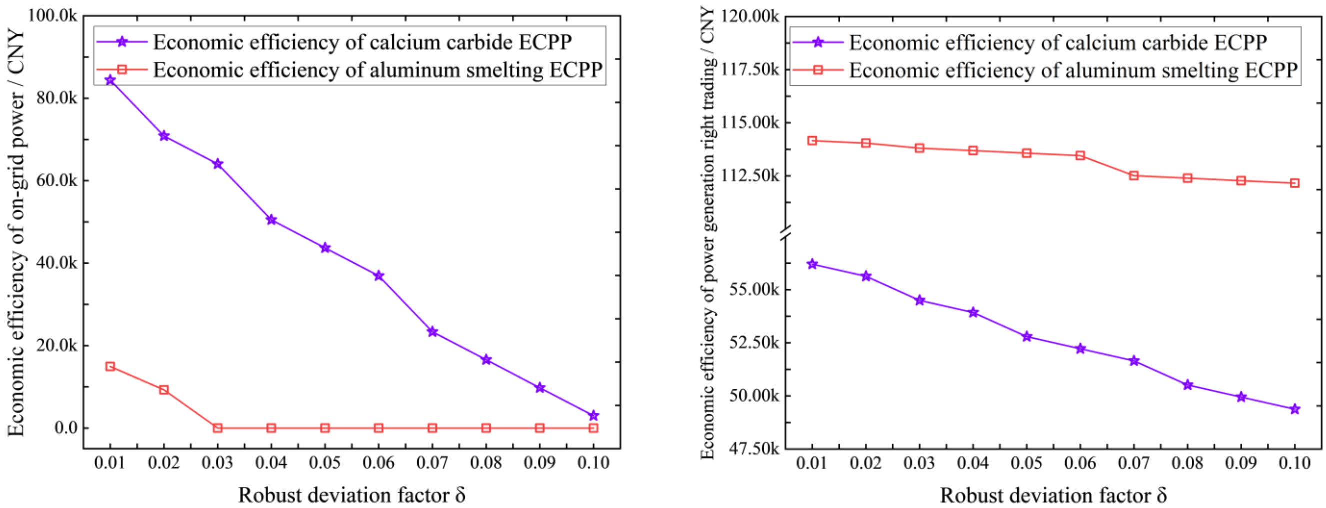

(**a**) Supply power to grid (**b**) Power generation rights trading

Figure 12. The economic efficiency trends of ECPPs.

From the perspective of on-grid power revenue, when the robust deviation factor increases to 0.1, the economic efficiency of on-grid power of the calcium carbide ECPP reaches a critical minimum. When the robust deviation factor is set to 0.03, aluminum-smelting ECPP's willingness to supply power to the grid decreases to 0. This is because the on-grid power capacity of the aluminum-smelting ECPP is smaller than that of the calcium carbide ECPP in the deterministic optimization results, resulting in a weaker anti-risk capability for the aluminum-smelting ECPP compared to the calcium carbide ECPP.

IGDT cannot improve the ECPP's willingness to supply power to the grid, but it helps the power grid system to become aware of the energy prices at which the ECPP is willing to participate in peak shaving and aids in the identification of ECPPs suitable for peak shaving.

In Figure 11, the two ECPPs both have renewable energy accommodation costs, indicating that power generation rights trading can still work when the robust deviation factor increases to 0.1. The trends of economic efficiency of ECPPs participating in power generation rights trading are shown in Figure 12b. The low economic benefit of the calcium carbide ECPP is due to its large unit capacity. Compared with the aluminum-smelting ECPP, the output value of the calcium carbide ECPP is still relatively high after reducing the output; therefore, its ability to resist risks in terms of new energy consumption is relatively weak.

During the process of power generation rights trading, due to the centralized bidding process between ECPPs and new energy enterprises, it is believed that the trading price of power generation rights is an uncertain factor with certain deterministic characteristics. Based on the deterministic optimization results, the critical trading prices for the calcium carbide ECPP and aluminum-smelting ECPP are 0.145 CNY/kWh and 0.336 CNY/kWh, respectively. If the trading price exceeds these prices, it will lead to a failed trade.

Among uncertain results, as the robustness factor increases, the willingness of ECPPs to participate in generation rights trading gradually decreases. With this disturbance factor, there arises the maximum uncertainty radii for three prices, indicating that when coal prices and carbon prices fluctuate within this corresponding radius, as long as the generation rights trading price does not exceed its fluctuation radius, power generation rights trading can be established, and this can also ensure that the ECPP remains profitable. This is because if the power generation rights trading fails, there will be no corresponding uncertainty radius.

Based on historical data, the strong volatility of coal and carbon prices are typically seen in the long-term market. However, in the short-term market (measured in per day), the price fluctuation range is relatively small. Through the analysis of IGDT, price changes can be covered. Therefore, when conducting IGDT analysis on the second day's data using the data from the current day, this method can be considered as effectively ensuring the success of power generation rights trading.

4.3.2. The Effect of Weight Coefficients on the Dispatching Results of the IGDT Model

In this paper, the robust deviation factor is set to 0.02, and different weight coefficients are selected to optimize the IGDT dispatching model. The results are shown in Tables 4 and 5.

Table 4. Calcium carbide ECPP's uncertainty radius with different weight coefficients.

ω_{coal}	ω_{co2}	$\omega_{N\text{-}G}$	α_{coal}	α_{co2}	$\alpha_{N\text{-}G}$	α	**Csum/CNY**
5	1	5	0.0062	0.0554	0.0238	0.23	2,060,581
5	1	10	0.0062	0.0561	0.0241	0.31	2,060,594
10	1	10	0.0063	0.0571	0.0246	0.38	2,060,605
10	1	15	0.0064	0.0589	0.0252	0.42	2,060,611
20	1	10	0.0064	0.0591	0.0253	0.4831	2,060,620

Table 5. Aluminum-smelting ECPP's uncertainty radius with different weight coefficients.

ω_{coal}	ω_{co2}	ω_{N-G}	α_{coal}	α_{co2}	α_{N-G}	α	**Csum/CNY**
5	1	5	0.013	0.0357	0.0384	0.3053	1,445,417
5	1	10	0.013	0.0357	0.0384	0.4759	1,445,417
10	1	10	0.0131	0.036	0.04	0.5669	1,445,923
10	1	15	0.0131	0.0361	0.0431	0.8137	1,446,285
20	1	10	0.0132	0.0363	0.0431	1.03	1,446,456

As can be seen from Tables 4 and 5, different weight coefficients can affect the results of the single uncertainty radius of coal price, carbon price, and power generation trading price. The size of the uncertainty radius is inversely correlated with the sensitivity of ECPP to price fluctuations. ECPPs can set the weight coefficient based on the principle that the higher the sensitivity, the higher the weight coefficient.

According to Tables 4 and 5, the fluctuation range of the total costs for both companies is not significant, which is due to the relatively small single uncertainty radius. However, the sensitivity of ECPPs to each price can be observed. The ECPPs both have the highest sensitivity to coal prices; since power generation rights trading prices have a certain degree of certainty, the sensitivity is relatively lower when compared to coal prices.

Comparing the uncertainty radius of the transaction prices of the two ECPPs, it can be seen that the radius of the calcium carbide ECPP is smaller, indicating a lower ability to resist risks after participating in power generation rights trading. Therefore, to ensure the success of generation rights trading, the ECPP needs to pay attention to its bidding price during the centralized bidding stage (especially when coal and carbon prices are already certain) and ensure that the trading price does not exceed the uncertainty radius that could lead to failed trading.

5. Conclusions

To encourage ECPPs to participate in power grid supply–demand regulation, this paper proposes a power generation and consumption optimization model of ECPPs based on a day-ahead and intra-day two-stage dispatching model and takes into account the impact of price uncertainty. By analyzing the optimization results of the proposed model, the conclusions are as follows:

(1) Under the two-stage dispatching model, ECPPs can better alleviate the supply and demand contradiction in the power system. At the same time, power generation rights trading and load regulation can be conducive to ECPPs' source-load decoupling to a certain extent and release more regulation potential. A segmented/sequential feedback solution strategy is beneficial for solving this.

(2) For high-energy-consumption enterprises with different industry categories, installed capacity and process characteristics, the power generation and consumption optimization model described in this paper can ensure their economic viability and promote their low-carbon development, as well as the safe and stable operation of the power grid system.

(3) Taking price uncertainty into account, ECPPs can maintain their own profitability during price fluctuations, and this could clarify the willingness of ECPPs to participate in regulation, which helps the power system grasp their regulatory potential. Meanwhile, IGDT contributes to ECPPs maintaining profitability in generation rights trading quotations.

Author Contributions: Conceptualization, H.L., H.Z. and D.P.; methodology, H.L., H.Z. and J.Y.; data curation, H.L. and J.Y.; formal analysis, H.L., H.Z. and J.Y.; validation, H.L., H.Z. and D.P.; writing—original draft preparation, H.L.; supervision, H.Z. and D.P.; writing—review and editing, H.Z. and D.P.; project administration/resources, D.P., H.Z. and J.Y. All authors have read and agreed to the published version of the manuscript.

Funding: This research was supported by the Science and Technology Project of the State Grid Corporation of China (5400-202236173A-1-1-ZN).

Data Availability Statement: Data is contained within the article.

Conflicts of Interest: Author Jincheng Yang was employed by the company State Grid Xinjiang Electric Power Co., Ltd. The remaining authors declare that the research was conducted in the absence of any commercial or financial relationships that could be construed as a potential conflict of interest. The authors declare that this study received funding from State Grid Corporation of China. The funder had the following involvement with the study: methodology, data curation, formal analysis and project administration/resources. All authors declare that the research was conducted without any commercial or financial activities or relationships that may be interpreted as potential conflicts of interest.

Appendix A

Table A1. Related parameters of ECPPs.

Parameter Name	Industry Category	Specific Data
Installed capacity/MW	Calcium carbide	2 × 300
	Aluminum smelting	2 × 150
Maximum and minimum technical output/MW	Calcium carbide	300, 175
	Aluminum smelting	150, 90
Ramp-up and ramp-down rates/(MW/min)	Calcium carbide	3, 3
	Aluminum smelting	2, 2
Unit consumption characteristic parameters a/(t/MW^2) b/(t/MW) c/t	Calcium carbide	0.00013 0.27601 16.00726
	Aluminum smelting	0.0004 0.2285 27.6206
Generation right shifting trading prices/(CNY/kWh)	Calcium carbide	0.1
	Aluminum smelting	0.13

Table A2. Install capacity of new energy power plants.

Type of New Energy Power Plant	Install Capacity/MW
Wing power plant	1383
Photovoltaic power station	650

Table A3. Time-of-use electricity price.

Period Type	Time	Electricity Price/(CNY/kWh)
Peak time period	8:00–11:00 19:00–24:00	0.700085
Normal time period	0:00–2:00 11:00–14:00 16:00–19:00	0.488259
Valley time period	2:00–8:00 14:00–16:00	0.176433

Table A4. Other price parameters related to the example.

Parameter Name	Specific Data
Benchmark on-grid price of thermal power $c_{u,t}$/(CNY/kWh)	0.22
Coal price c_{coal}/(CNY/t)	350
Carbon price c_{co2}/(CNY/t)	56
Transmission–distribution price $c_{t,d}$/(CNY/kWh)	0.0738
Government funds and surcharges c_{gov}/(CNY/kWh)	0.0041
Self-generated electricity emission factor $k_{G,t}$	0.9
Purchased electricity emission factor $k_{d,t}$	0.2
Compensation price of load reduction (day-ahead) ζ_D/(CNY/kWh)	0.15
Compensation price of load reduction (intra-day) ζ_D/(CNY/kWh)	0.3

Table A5. Other price parameters related to load reduction.

Task Number	λ_m	Reduction Level	$T^{on}_{Dm,min}$, $T^{on}_{Dm,max}$
1	4.14	3	0, 8
5	0.8	2	0, 6

Table A6. Parameters of the PSP.

Parameter Name	Specific Data
Water volume to electricity conversion coefficient (Pumping and generation), η_p, $\eta_g/(m^3/MWh)$	561.75, 748.5
$P^{g,min}_{psp,j,t}$, $P^{g,max}_{psp,j,t}$, $P^{g,min}_{psp,j,t}$, $P^{g,max}_{psp,j,t}$/MW	0, 300 0, 300
Upper and lower limits of upstream reservoir storage capacity $S_{psp,min}(S_0)$, $S_{psp,max}$ /$(10^4 m^3)$	71.46, 190

Appendix B

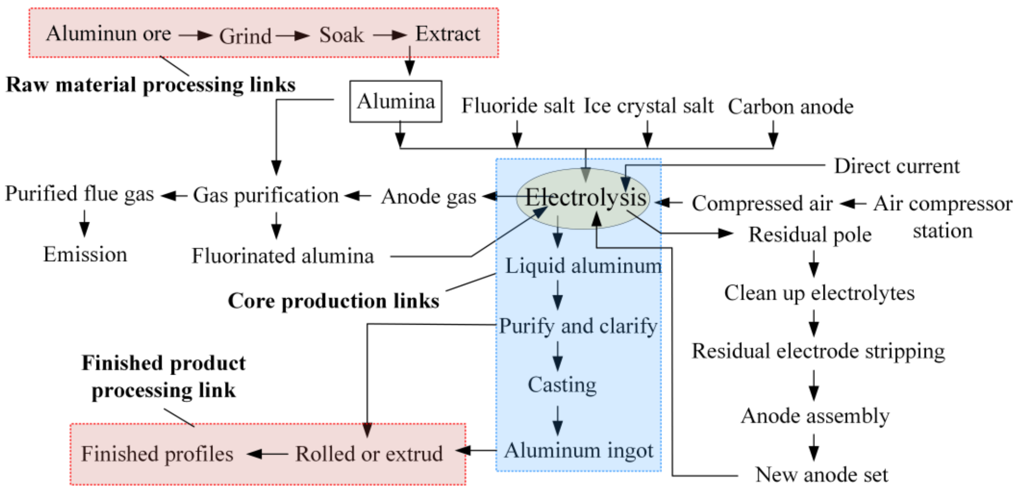

Figure A1. Aluminum-smelting ECPP's production process flow.

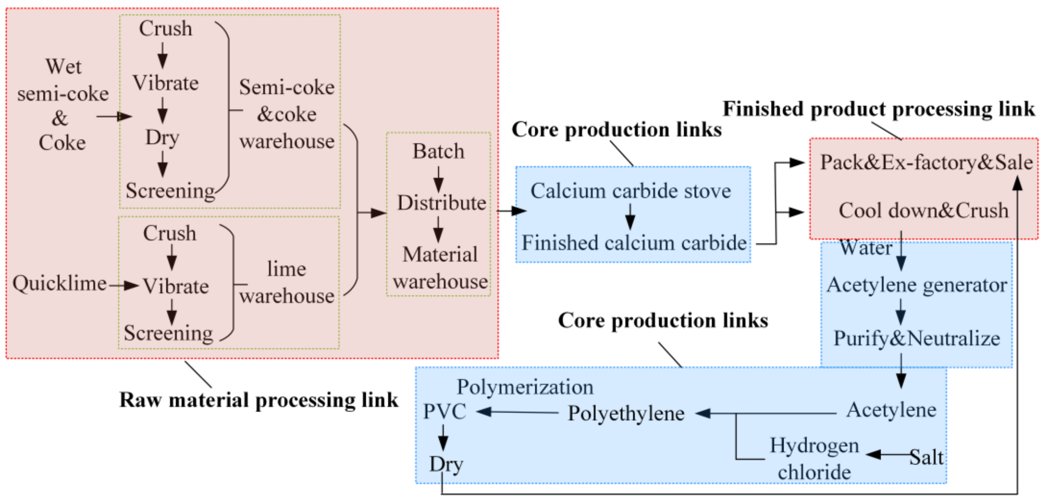

Figure A2. Calcium carbide ECPP's production process flow.

Appendix C

The specific trading process of the power generation right is as follows:

The two parties involved in the power generation rights trading (captive power plants and renewable energy enterprises) submit their respective data, including trading electricity volume and trading quotes, on the platform of the EPTC. Matching is then conducted based on the trading rule of high–low matching. The offering prices declared by the ECPP are sorted from high to low to form a seller sequence (which refers to the selling of power generation rights, rather than electricity quantity), while the bid prices declared by renewable energy enterprises are sorted from low to high to form a buyer sequence. Matching pairs are formed from the highest seller and the lowest buyer, proceeding in sequence until the difference between the buyer's and seller's prices exceeds or equals 0. The trading process is shown in Table A7.

Table A7. Matrix table of bidding price differences in power generation rights trading.

	I_1	I_2	...	I_m
J_1	$P_{j1} - P_{i1}$	$P_{j1} - P_{i2}$	...	$P_{j1} - P_{im}$
J_2	$P_{j2} - P_{i1}$	$P_{j2} - P_{i2}$	...	$P_{j2} - P_{im}$
...	...	...	...	...
J_{n}	$P_{jn} - P_{i1}$	$P_{jn} - P_{i2}$		$P_{jn} - P_{im}$

The horizontal axis represents the ECPPs, while the vertical axis represents renewable energy enterprises. The matrix encompasses all possible trading pairs and the bidding price differences for each pair, facilitating the determination of the search scope for trading pairs. Select the maximum element in Table A7 that satisfies the trading conditions, and the final trading price will be the average of the bids of both parties. The bundling policy is adopted for renewable energy sources; thus, there is only one vertical coordinate in Table A7.

Appendix D

The constraints that need to be considered in the dispatching process of the power grid system for PSPs are as follows:

$$\begin{cases} P^{\mathrm{g,min}}_{\mathrm{psp},j,t} x_{\mathrm{p},j,t} \le P^{\mathrm{g}}_{j,t} \le P^{\mathrm{g,max}}_{\mathrm{psp},j,t} x_{\mathrm{p},j,t}, \;\; P^{\mathrm{g,min}}_{\mathrm{psp},j,t} y_{\mathrm{p},j,t} \le P^{\mathrm{g}}_{j,t} \le P^{\mathrm{g,max}}_{\mathrm{psp},j,t} y_{\mathrm{p},j,t} \\ x_{\mathrm{p},j,t} \le N_k \delta^{\mathrm{g}}_{j,t}, \;\; y_{\mathrm{p},j,t} \le N_k \delta^{\mathrm{p}}_{j,t}, \;\; \delta^{\mathrm{g}}_{j,t} + \delta^{\mathrm{p}}_{j,t} \le 1 \\ S_{\mathrm{psp,min}} \le S_t \le S_{\mathrm{psp,max}}, \;\; S_0 - S_T = 0 \\ S_{t+1} = S_t + \sum\limits_{j \in N_k} (P^{\mathrm{g}}_{j,t} \eta_{\mathrm{g}} - P^{\mathrm{p}}_{j,t} \eta_{\mathrm{p}}) \times \Delta t \end{cases}$$

where $P^{\mathrm{g,min}}_{\mathrm{psp},j,t}$, $P^{\mathrm{g,max}}_{\mathrm{psp},j,t}$ and $P^{\mathrm{g,min}}_{\mathrm{psp},j,t}$, $P^{\mathrm{g,max}}_{\mathrm{psp},j,t}$ are the lower and upper limits of the power generation and pumping power of the PSP units, respectively; $x_{\mathrm{p},j,t}$, $y_{\mathrm{p},j,t}$ are Boolean variables for power generation and water pumping, respectively; $\delta^{\mathrm{g}}_{j,t}$ and $\delta^{\mathrm{p}}_{j,t}$ are the power generation and pumping states of the PSP, respectively; $S_{\mathrm{psp,min}}$ and $S_{\mathrm{psp,max}}$ are the maximum and minimum storage capacities of the upper reservoir, respectively; S_t is the storage capacity of the upper reservoir at time t of the PSP; S_0 is the initial storage capacity of the upper reservoir; and η_{g} and η_{p} are the conversion coefficients of water and electricity for power generation and pumping, respectively.

References

1. Baležentis, T.; Štreimikiene, D. Sustainability in the electricity sector through advanced technologies: Energy mix transition and smart grid technology in China. *Energies* **2019**, *12*, 1142. [CrossRef]
2. He, S.J.; Liu, Y.J. Optimal Allocation Stochastic Model of Distributed Generation Considering Demand Response. *Energies* **2024**, *17*, 795. [CrossRef]
3. Williams, B.; Bishop, D.; Gallardo, P.; Chase, J.G. Demand Side Management in Industrial, Commercial, and Residential Sectors: A Review of Constraints and Considerations. *Energies* **2023**, *16*, 5155. [CrossRef]
4. Golmohamadi, H. Demand-side management in industrial sector: A review of heavy industries. *Renew. Sust. Energ. Rev.* **2022**, *156*, 111963. [CrossRef]
5. Abdul-Majeed, M.A.; Al-Hadhrami, L.M.; Al-Soufi, K.Y.; Ahmad, F.; Rehman, S. Captive power generation in saudi arabia-overview and recommendations on policies. *Energy. Policy* **2013**, *62*, 379–385. [CrossRef]
6. Naqvi, S.R.; Naqvi, M.; Taqvi, S.A.A.; Iqbal, F.; Inayat, A.; Khoja, A.H.; Mehran, M.T.; Ayoub, M.; Shahbaz, M.; Amin, N.A.S. Agro-industrial residue gasification feasibility in captive power plants: A South-Asian case study. *Energy* **2021**, *214*, 118952. [CrossRef]
7. Goswami, U.; Sadju, P.K.; Chakraborty, S. Enhancement of controllability to improve the transient performance for captive power plant in islanding condition: A case of study. *Int. J. Electr. Power Energy Syst.* **2016**, *83*, 188–202. [CrossRef]

8. Liu, J.; Huang, X.X.; Liu, X.L.; Han, Z.L. Research on Energy Management Strategy of Captive Power Plant Based on Hybrid. *Method Sens.* **2019**, *31*, 2155–2165.
9. Ramin, D.; Spinelli, S.; Brusaferri, A. Demand-side management via optimal production scheduling in power-intensive industries: The case of metal casting process. *Adv. Technol. Electr. Eng. Energy* **2018**, *225*, 622–636. [CrossRef]
10. Adesanya, A.A.; Pearce, J.M. Econnmic viability of captive off-grid solar photovoltaic and diesel hybrid energy systems for the Nigerian private sector. *Renew. Sustain. Energy Rev.* **2019**, *114*, 109348. [CrossRef]
11. Bagdadee, A.H.; Zhang, L. Power Quality Impact on the Industrial Sector: A Case Study of Bangladesh. *J. Electr. Eng. Technol.* **2019**, *14*, 1841–1857. [CrossRef]
12. Afandi, A.N.; Gumilar, L.; Fadlika, I. Local Power Grid Assessment of the Power System Expansion Considering Captive Power Plants. In Proceedings of the 4th International Conference on Industrial, Mechanical, Electrical, and Chemical Engineering, Surakarta, Indonesia, 9–11 October 2018; p. 030072.
13. Peng, B.Y.; Zhao, H.F.; Bai, J.M.; Wang, W.Z. Study on Solution of Renewable Energy Accommodation Based on Quantitative Analysis Model. In Proceedings of the 3th International Conference on Smart Power and Internet Energy Systems (SPIES), Shanghai, China, 25–28 September 2021; pp. 414–420.
14. Ali, A.; Innocent, K. Energy management in microgrids using transactive energy control concept under high penetration of Renewables; A survey and case study. *Renew. Sustain. Energy Rev.* **2023**, *176*, 113161.
15. Qi, H.; Waqas, A.; Khalid, U.; Hoay, B.G.; Foo, Y.S.E.; Muhammad, A.; Mahnoor, S.; Abdullah, A.K.; Syed, A.A. A review of transactive energy systems: Concept and implementation. *Energy Rep.* **2021**, *7*, 7804–7824.
16. Lucas, S.M.; Fernando, L.T.; Diego, I.; Marcos, E.P.M.; Giovanni, C.B.; Raimundo, F.S.; Ruth, P.S.L. Co-simulation platform for the assessment of transactive energy systems. *Electr. Power. Syst. Res.* **2023**, *233*, 109693.
17. PAULUS, M.; BORGGREFE, F. The potential of demand-side management in energy-intensive industries for electricity market in Germany. *Appl. Energy* **2011**, *88*, 432–441. [CrossRef]
18. Wang, Z.J.; Gao, F.; Zhai, Q.Z.; Guan, X.H.; Wu, J.; Liu, K. Electrical Load Tracking Analysis for Demand Response in Energy Intensive Enterprise. *IEEE Trans. Smart Grid.* **2013**, *4*, 1917–1927. [CrossRef]
19. Reddy, B.K.; Singh, A.K. Optimal Operation of a Photovoltaic Integrated Captive Cogeneration Plant with a Utility Grid Using Optimization and Machine Learning Prediction Methods. *Energies* **2021**, *14*, 4935. [CrossRef]
20. Mohanta, D.K.; Sadhu, P.K.; Chakrabarti, R. Deterministic and stochastic approach for safety and reliability optimization of captive power plant maintenance scheduling using GA/SA-based hybrid techniques: A comparison of results. *Reliab. Eng Syst. Saf.* **2007**, *92*, 187–199. [CrossRef]
21. Kunche, A.; Mielczarek, B. Application of System Dynamic Modelling for Evaluation of CO_2 Emissions and Expenditure for Captive Power Generation Scenarios in the Cement Industry. *Energies* **2021**, *14*, 3115. [CrossRef]
22. Zhang, S.R.; Zhang, J.; Cheng, L.; Wang, Z.B.; Li, W.; Liu, C. A bi-level framework for interactive competition and CPPs-based demand response. *J. Renew. Sustain. Energy* **2023**, *15*, 035502. [CrossRef]
23. Mahmood, A. Gazing Lean through the lens of System of Systems Dynamics: A case of weaving mill. *J. Eng. Fibers Fabr.* **2019**, *14*, 155892501987070. [CrossRef]
24. Xu, J.H.; Du, Y.L.; Cui, H.J.; Yin, Z.; Zhang, Z.; Ma, F.; Tan, C.; Lou, T.Y. Research on alternative electricity calculation method of alternative transaction between new energy and captive power plant. *J. Phys. Conf. Ser.* **2018**, *1087*, 022029. [CrossRef]
25. Li, S.T.; Zhang, S.F.; Andrews-Speed, P. Using diverse market-based approaches to integrate renewable energy: Experiences from China. *Energy Policy* **2019**, *125*, 330–337. [CrossRef]
26. He, Y.X.; Pang, Y.X.; Guan, J. A TOU Pricing Mechanism to Promote Renewable Energy Consumption: The Case of the Western Inner Mongolia Grid in China. *Math. Probl. Eng.* **2017**, *2017*, 9454358. [CrossRef]
27. Liu, H.H.; You, D.N.; Cai, Y.B.; Zhang, G.Q.; Wang, H.; Zhang, L. Peak shaving market mechanism of captive power plants considering energy consumption characteristics of enterprises. In Proceedings of the 2021 International Conference on Power System Technology: Carbon Neutrality and New Type of Power System, Haikou, China, 8–9 December 2021; pp. 720–724.
28. Liu, Z.D.; Nazari-Heris, M. Optimal bidding strategy of multi-carrier systems in electricity markets using information gap decision theory. *Energy* **2023**, *280*, 128043. [CrossRef]
29. Naghdehforoushha, M.; Fooladi, M.D.T.; Rezvani, M.H.; Sadeghi, M.M.G. A robust model for spot virtual machine bidding in the cloud market using information gap decision theory (IGDT). *Turk. J. Electr. Eng. Comput. Sci.* **2023**, *31*, 193–215. [CrossRef]
30. Hosseini, S.E.; Najafi, M.; Akhavein, A.; Shahparasti, M. Day-Ahead Scheduling for Economic Dispatch of Combined Heat and Power With Uncertain Demand Response. *IEEE Access* **2022**, *10*, 42441–42458. [CrossRef]